AGU PUBLICATIONS

JGR

Journal of Geophysical Research: Biogeosciences

RESEARCH ARTICLE

10.1002/2016JG003615

Key Points:
- Quantify discharge of suspended sediment and particulate organic carbon (biospheric and petrogenic) by an Andean River
- The fate of river biospheric particulate organic carbon determines whether Andean forest is a carbon dioxide source or sink
- Oxidation of petrogenic particulate organic carbon eroded from the Andes counters CO_2 drawdown by silicate weathering in the lowlands

Supporting Information:
- Supporting Information S1
- Data Set S1

Correspondence to:
K. E. Clark,
kathryn.clark23@gmail.com

Citation:
Clark, K. E., R. G. Hilton, A. J. West, A. Robles Caceres, D. R. Gröcke, T. R. Marthews, R. I. Ferguson, G. P. Asner, M. New, and Y. Malhi (2017), Erosion of organic carbon from the Andes and its effects on ecosystem carbon dioxide balance, *J. Geophys. Res. Biogeosci.*, *122*, doi:10.1002/2016JG003615.

Received 6 SEP 2016
Accepted 16 JAN 2017
Accepted article online 24 JAN 2017

Erosion of organic carbon from the Andes and its effects on ecosystem carbon dioxide balance

K. E. Clark[1,2], R. G. Hilton[3], A. J. West[4], A. Robles Caceres[5], D. R. Gröcke[6], T. R. Marthews[1,7], R. I. Ferguson[3], G. P. Asner[8], M. New[9,10], and Y. Malhi[1]

[1]Environmental Change Institute, School of Geography and the Environment, University of Oxford, Oxford, UK, [2]Department of Earth and Environmental Science, University of Pennsylvania, Philadelphia, Pennsylvania, USA, [3]Department of Geography, Durham University, Durham, UK, [4]Department of Earth Sciences, University of Southern California, Los Angeles, California, USA, [5]Facultad de Ciencias Biológicas, Universidad Nacional de San Antonio Abad del Cusco, Cusco, Peru, [6]Department of Earth Sciences, Durham University, Durham, UK, [7]Centre for Ecology and Hydrology, Wallingford, UK, [8]Department of Global Ecology, Carnegie Institution for Science, Stanford, California, USA, [9]African Climate and Development Initiative, University of Cape Town, Rondebosch, South Africa, [10]School of International Development, University of East Anglia, Norwich, UK

Abstract Productive forests of the Andes are subject to high erosion rates that supply to the Amazon River sediment and carbon from both recently photosynthesized biomass and geological sources. Despite this recognition, the source and discharge of particulate organic carbon (POC) in Andean Rivers remain poorly constrained. We collected suspended sediments from the Kosñipata River, Peru, over 1 year at two river gauging stations. Carbon isotopes (^{14}C, ^{13}C, and ^{12}C) and nitrogen to organic carbon ratios of the suspended sediments suggest a mixture of POC from sedimentary rocks (POC_{petro}) and from the terrestrial biosphere ($POC_{biosphere}$). The majority of the $POC_{biosphere}$ has a composition similar to surface soil horizons, and we estimate that it is mostly younger than 850 ^{14}C years. The suspended sediment yield in 2010 was $3500 \pm 210\ t\ km^{-2}\ yr^{-1}$, >10 times the yield from the Amazon Basin. The $POC_{biosphere}$ yield was $12.6 \pm 0.4\ t\ C\ km^{-2}\ yr^{-1}$ and the POC_{petro} yield was $16.1 \pm 1.4\ t\ C\ km^{-2}\ yr^{-1}$, mostly discharged in the wet season (December to March) during flood events. The river $POC_{biosphere}$ discharge is large enough to play a role in determining whether Andean forests are a source or sink of carbon dioxide. The estimated erosional discharge of POC_{petro} from the Andes is much larger (~1 Mt C yr^{-1}) than the POC_{petro} discharge by the Madeira River downstream in the Amazon Basin, suggesting that oxidation of POC_{petro} counters CO_2 drawdown by silicate weathering. The flux and fate of Andean $POC_{biosphere}$ and POC_{petro} need to be better constrained to fully understand the carbon budget of the Amazon River basin.

1. Introduction

Tropical forests and soils contain ~430 Pg C stored within organic matter [*Dixon et al.*, 1994; *Houghton*, 2005; *Saatchi et al.*, 2011], which is >70% of the carbon dioxide (CO_2) stock of the preindustrial atmospheric reservoir [*Sundquist and Visser*, 2004]. Physical erosion can export some of this biospheric carbon and supply it to river systems, which globally deliver $0.16 + 0.07/-0.05\ Pg\ C\ yr^{-1}$ of particulate organic carbon ($POC_{biosphere}$) to the oceans [*Galy et al.*, 2015]. Over short time scales (10^0–10^3 years), this is an export of net primary production from ecosystems [*Seitzinger et al.*, 2005; *Mayorga et al.*, 2010; *Galy et al.*, 2015]. If the eroded $POC_{biosphere}$ is replaced by new productivity, erosion is a net sink of atmospheric CO_2 [*Stallard*, 1998; *Berhe et al.*, 2007; *Li et al.*, 2015]. Over longer time scales ($>10^3$ years), the eroded $POC_{biosphere}$ may be buried in continental or marine sedimentary deposits, where it becomes a geological CO_2 sink [*Berner*, 1982; *France-Lanord and Derry*, 1997; *Stallard*, 1998; *Galy et al.*, 2007b; *Kao et al.*, 2014]. Alternatively, oxidation of $POC_{biosphere}$ during transit through river basins can fuel ecosystems downstream [*Mayorga et al.*, 2005] and is a component of heterotrophic respiration, which is not included in ecosystem carbon budgets at the scale of forest plots [*Malhi*, 2012]. If the carbon is old, such as carbon stored over millennial time scales in soils [*Galy and Eglinton*, 2011; *Hilton et al.*, 2015] and over longer time scales in sedimentary rocks as "petrogenic" POC (POC_{petro}) [*Galy and Eglinton*, 2011; *Hilton et al.*, 2011a], its oxidation represents a source of CO_2 to the atmosphere not captured in most budgets [*Bouchez et al.*, 2010; *Hilton et al.*, 2014; *Vihermaa et al.*, 2014].

High rates of physical erosion occur in mountains [*Milliman*, 1995; *Kao and Liu*, 1997; *Hicks et al.*, 2000; *Lyons et al.*, 2002; *Hilton et al.*, 2008a; *Wheatcroft et al.*, 2010; *Milliman and Farnsworth*, 2011; *Hilton et al.*, 2012; *Goñi*

et al., 2013; *Larsen et al*., 2014], and because of the association between POC and clastic sediment, these locations also experience the highest measured rates of POC discharge [*Milliman*, 1995; *Kao and Liu*, 1997; *Hicks et al*., 2000; *Lyons et al*., 2002; *Hilton et al*., 2008a; *Wheatcroft et al*., 2010; *Milliman and Farnsworth*, 2011; *Hilton et al*., 2012; *Stallard*, 2012; *Goñi et al*., 2013; *Hilton*, 2017]. Rivers draining mountain islands can export this POC efficiently to ocean basins [*Hilton et al*., 2008a; *Wheatcroft et al*., 2010; *Kao et al*., 2014]. However, many mountain rivers drain to larger continental river systems, and their POC and sediment are instead transported for thousands of kilometers across floodplains [e.g., *Galy et al*., 2008b; *Blair and Aller*, 2012; *Bouchez et al*., 2014; *Moreira-Turcq et al*., 2014].

The Amazon Basin (~6×10^6 km^2 catchment area) has much of its headwaters in the Andes, which cover ~600,000 km^2 but are thought to supply most of the 550–1550 Mt yr^{-1} of clastic sediment exported to the Atlantic Ocean [e.g., *Gibbs*, 1967; *Meade et al*., 1979; *Richey et al*., 1986; *Allegre et al*., 1996; *Dunne et al*., 1998; *Guyot et al*., 2005; *Filizola and Guyot*, 2009; *Martinez et al*., 2009]. Many studies have measured POC composition and discharge in the Amazon Basin [e.g., *Richey et al*., 1990; *Moreira-Turcq et al*., 2003; *Bouchez et al*., 2014; *Feng et al*., 2016] and within Andean tributaries [e.g., *Hedges et al*., 2000; *Aufdenkampe et al*., 2007; *Townsend-Small et al*., 2007; *Townsend-Small et al*., 2008; *Clark et al*., 2013]. Recent work has highlighted the importance of rock-derived POC_{petro} input to Andean Rivers [*Bouchez et al*., 2010; *Clark et al*., 2013; *Bouchez et al*., 2014]. However, the rates of $POC_{biosphere}$ and POC_{petro} discharges in this setting are not well known, hampering efforts to link Andean erosion to carbon budgets over interannual time scales. Quantifying POC discharge is essential in order to understand the context and mechanisms that constrain Andean net ecosystem productivity because the transport of carbon from the Andes to the Amazon Basin and the Atlantic Ocean represents a substantial carbon flux, of similar magnitude to the net carbon balance of the Amazon forest ecosystem, which forest inventory studies suggest accounts for around 25% of global terrestrial carbon sequestration [*Malhi*, 2010].

We aim to provide new insight into the impact of physical erosion on carbon budgets by quantifying the source and magnitude of river discharge of POC from the steep, eastern flank of the Peruvian Andes, characterized by predominantly sedimentary bedrock with relatively high concentrations of petrogenic organic carbon. We focus on a catchment where previous work has established the hydrological water balance [*Clark et al*., 2014]; rates of geomorphic processes such as landslides [*Clark et al*., 2016]; and forest productivity, respiration, and carbon stocks across the landscape [*Zimmermann et al*., 2009; *Zimmermann et al*., 2010a; *Marthews et al*., 2012; *Girardin et al*., 2014b; *Clark et al*., 2016; *Malhi et al*., 2016]. We use a detailed set of suspended sediment samples and hydrometric river gauging measurements over a 12 month period and analyze the stable isotopes of POC ($\delta^{13}C_{org}$), the nitrogen to organic carbon ratio ([N]/[OC_{total}]), and the radiocarbon activity of POC to distinguish POC_{petro} derived from sedimentary rocks and to study the source and age of $POC_{biosphere}$. We evaluate how the erosion of carbon from the terrestrial biosphere impacts estimates of Andean net ecosystem productivity and assess the role of Andean $POC_{biosphere}$ and POC_{petro} in the longer-term carbon cycle.

2. Study Area

The Kosñipata River is located in the Eastern Cordillera of the central Peruvian Andes (Figure 1). The steep topography [*Montgomery et al*., 2001] originated from moderate rates of surface uplift of 0.2–0.3 mm yr^{-1} due to plate convergence and subduction of the Nazca Plate under the South American Plate [*Gregory-Wodzicki*, 2000]. The South American low-level jet, which carries humid winds westward over the Amazon Basin [*Marengo et al*., 2004], is redirected by the Andes, driving the high annual precipitation up to 7000 mm yr^{-1} in parts of the eastern Andes [*Killeen et al*., 2007]. The climate and tectonic setting combine to produce moderate-to-high denudation rates of ~0.4 mm yr^{-1} in the central Andes according to cosmogenic radionuclide concentrations in detrital quartz [*Wittmann et al*., 2009] and decadal river gauging [*Guyot et al*., 1996]. The slopes are steep and prone to landslides, which harvest sediment and POC [*Blodgett and Isacks*, 2007; *Clark et al*., 2016]. In this part of the Andes, rivers drain large areas of sedimentary and meta-sedimentary melanges that comprise ~80% of the Kosñipata River drainage area [*Clark et al*., 2013].

The Kosñipata River is a tributary of the Madre de Dios River which feeds the Madeira River, a major Amazon tributary (Figures 1c and 1d). The wet climate sustains tropical montane cloud forest over 80% of the Kosñipata Basin (Figure 1a) [*Malhi et al*., 2010]. The catchment is located in Manu National Park and the adjacent buffer zone (Table 1). The forest contains significant stores of organic carbon (total

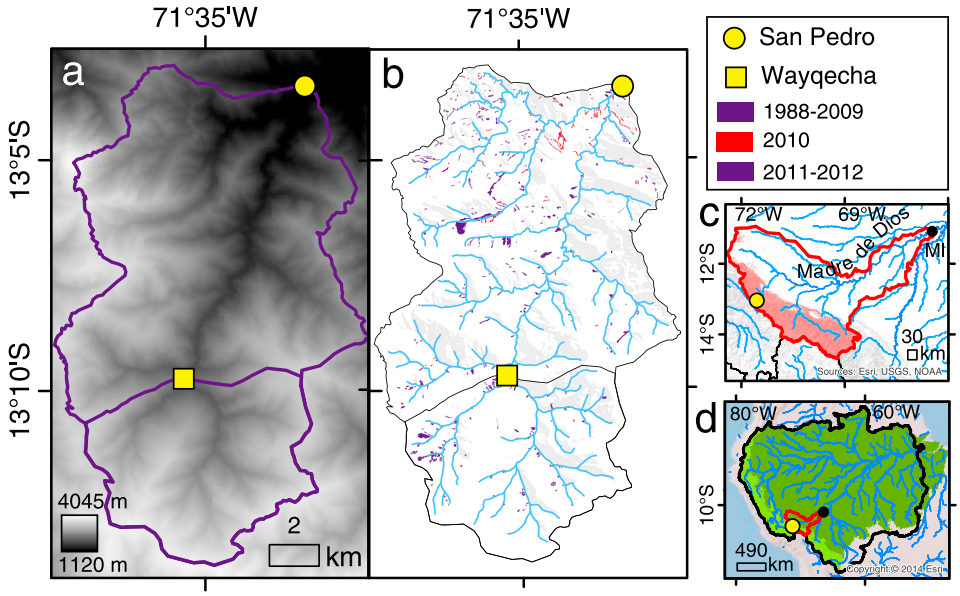

Figure 1. The Kosñipata River in the Peruvian Andes. (a) San Pedro gauging station (yellow circle) and catchment area (purple line) and the subcatchment at the Wayqecha gauging station (yellow square) overlain on topography from the Shuttle Radar Topographic Mission (SRTM) digital elevation model at 90 × 90 m resolution. (b) Landslides were mapped from satellite imagery at annual resolution from 1988 to 2012, for nontopographic shadow areas (shown in light grey, where landslides were not visible) [*Clark et al.*, 2016]. (c) The Kosñipata River feeds the Madre de Dios River (basin outlined in red), a tributary of the Madeira River draining to the Amazon River. The Miraflores gauging station (MI; black circle) captures a 124,000 km^2 catchment, of which the Andean portion of the Madre de Dios Basin (>550 m asl red shaded region) is 35,600 km^2. The river network was produced from HydroSHEDS [*Lehner et al.*, 2008]. (d) The Amazon River network with the Andes site (yellow circle) and the Miraflores River gauging station. The Andean portion of Amazonia (light green) and Amazonia in a strict sense (dark green) from *Eva et al.* [2005] fall mostly within the Amazon Basin (within black outline) [*Lehner et al.*, 2008].

35,000 ± 5000 t C km^{-2}), with 28,000 ± 4000 t C km^{-2} in soils and 5300 ± 800 t C km^{-2} in vegetation [*Clark et al.*, 2016]. Total carbon stocks increase slightly with elevation due to an increase of soil stocks and woody necromass with elevation, accompanied by a smaller reduction in standing live biomass [*Zimmermann et al.*, 2010b; *Gurdak et al.*, 2014; *Clark et al.*, 2016].

Table 1. Characteristics of Gauging Stations on the Kosñipata River, Peru, and Estimates of Suspended Load Yields Over the Water Year of Study (February 2010 to January 2011)

Gauging Station	San Pedro	Wayqecha
Location	13°3′37″, 71°32′40″	13°9′46″, 71°35′21″
Catchment area[a] (km^2)	164.4	48.5
Mean catchment slope[a] (deg)	28	26
Mean catchment elevation[a] (m)	2805	3195
Land cover[b]	TMCF (80%), puna/transition (20%)	TMCF (50%), puna/transition (50%)
Geology[c]	Mudstones (80%), pluton intrusions (20%)	Mudstones (100%)
Number of samples	68	46
Annual runoff[d] (mm yr^{-1})	2800 ± 130	3000 ± 1500
Suspended sediment yield[e] (t km^{-2} yr^{-1})	3500 ± 210 (2220 ± 130)	1270 ± 630
$POC_{biosphere}$ yield[e] (t C km^{-2} yr^{-1})	12.6 ± 0.4 (7.1 ± 0.2)	5.3 ± 2.7
POC_{petro} yield[e] (t C km^{-2} yr^{-1})	16.1 ± 1.4 (7.2 ± 0.9)	3.5 ± 1.8

[a]Based on Shuttle Radar Topography Mission (SRTM) data with a 90 m x 90 m resolution.
[b]Determined using 2009 Quickbird 2 imagery, where TMCF is the tropical montane cloud forest.
[c]Basin geology derived from *Carlotto Caillaux et al.* [1996].
[d]From *Clark et al.* [2014]. Annual runoff is more uncertain at Wayqecha as it is based on monthly averaged data.
[e]From this study. For San Pedro, yields are derived from rating curves (Figure 5) applied to continuous water discharge data (Figure 2). Values are corrected for log-transformed bias [*Ferguson*, 1986]. Values in brackets are nonbias corrected. For Wayqecha, yields are derived from monthly averaged data.

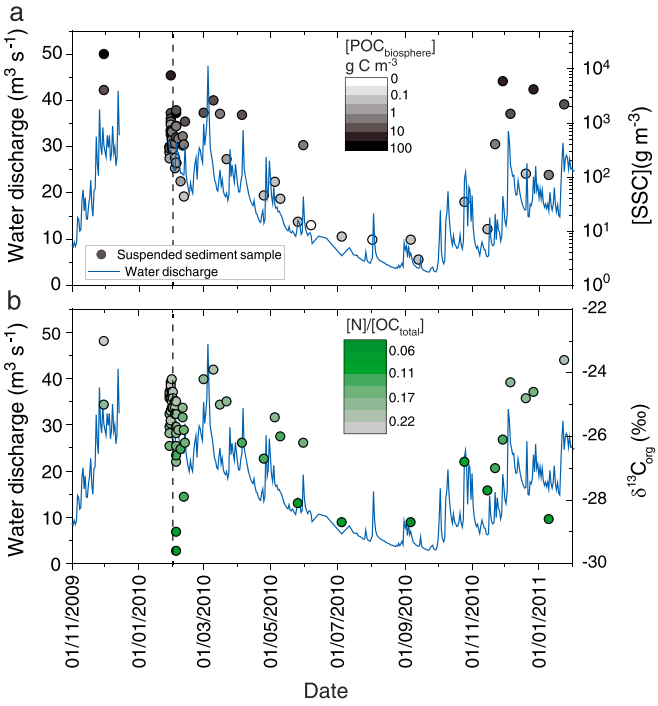

Figure 2. Sample collection and hydrometric measurements from the San Pedro gauge, Kosñipata River. (a) River water discharge (blue line; $m^3\ s^{-1}$) over the study period [*Clark et al.*, 2014] with suspended sediment samples (circles) and the corresponding suspended sediment concentration (SSC; $g\ m^{-3}$; right axis). The color of the circle corresponds to the estimated biospheric particulate organic carbon concentration ($POC_{biosphere}$; $g\ C\ m^{-3}$). (b) Same as in Figure 2a but with the stable isotope composition ($\delta^{13}C_{org}$; right axis) of the samples. The color of the fill is the nitrogen to organic carbon ratio ($[N]/[OC_{total}]$). The vertical dotted line illustrates the start of the year over which annual discharges and yields were calculated (Table 1).

The geology of the Kosñipata Valley is ~80% Paleozoic (~450 Ma) metasedimentary mudstones which contain POC_{petro}, with plutonic intrusions contributing the remaining ~20% of the catchment area [*Carlotto Caillaux et al.*, 1996] (Table 1). The geological characteristics are representative of the Andean portion of the Madre de Dios Basin [*Carlotto Caillaux et al.*, 1996; *El Instituto Geológico Minero y Metalúrgico*, 2013], covering approximately ~35,600 km^2.

Suspended sediment samples were collected between November 2009 and February 2011 from two gauging stations, one capturing the catchment of the Kosñipata River at San Pedro (1360 m above sea level (asl), 164.4 km^2; hereafter the "San Pedro" site) and the other the Wayqecha subbasin (2250 m asl, 48.5 km^2; hereafter the "Wayqecha" site) (Table 1 and Figure 1a). In this study, we greatly expand on the work of *Clark et al.* [2013], which investigated the source of POC during two storm events in January and February 2010 and demonstrated that POC_{petro} can contribute between ~10% and 80% of the total POC [*Clark et al.*, 2013].

Rainfall in the Kosñipata River valley ranges from 5300 mm yr^{-1} around the San Pedro gauging station to 1560 mm yr^{-1} in the high elevations of the Wayqecha sub-catchment [*Girardin et al.*, 2014b; *Huaraca Huasco et al.*, 2014]. Average basin-wide rainfall is 3112 ± 414 mm yr^{-1}, with an additional ~10% cloud water contribution to river runoff [*Clark et al.*, 2014]. The wet season is from December to March, the wet-dry transition season is April, the dry season is May to September, and the dry-wet transition season is October and November [*Clark et al.*, 2014]—although we note that there is still considerable rainfall during the dry season. Stream runoff at the San Pedro gauging station has been calculated over a water year with continuous data spanning 2010–2011, as 2796 ± 126 mm yr^{-1} (Table 1).

3. Materials and Methods

3.1. Sample Collection and Hydrometric Measurements

At the San Pedro and Wayqecha catchment outlets (Figure 1a), suspended sediment (SS) samples were collected for geochemical analysis from November 2009 to February 2011, which covers the majority of two wet seasons (Figure 2). Thirty-seven river SS samples were collected from San Pedro and 25 samples from Wayqecha at a weekly to monthly frequency. We combine this new data set with published data from a 2 week intensive sampling scheme in the 2010 wet season, when SS samples were collected every 3 hours at San Pedro ($n = 31$) and Wayqecha ($n = 21$), as described in *Clark et al.* [2013]. This takes the total number of SS samples used in this study (Table S1 in the supporting information) to 68 at San Pedro and 46 at Wayqecha (Table 1). The sampling strategy was designed to provide suspended sediments from a range of water discharges (Q_w; $m^3\ s^{-1}$), including flood events, in order to quantify SS, $POC_{biosphere}$, and POC_{petro}

discharges, following previous work in mountain rivers [*Hilton et al*., 2008b; *Kao and Milliman*, 2008; *Townsend-Small et al*., 2008].

At the San Pedro site, the Q_w at the times of sample collection varied from 5.9 to 42.4 $m^3 s^{-1}$ [*Clark et al*., 2014]. The full Q_w record was determined using an empirical relationship between stage height and Q_w measured at discrete times; this stage-discharge calibration was applied to the continuous stage height record [*Clark et al*., 2014]. At the Wayqecha gauging station, the Q_w varied from 2.3 $m^3 s^{-1}$ to 8 $m^3 s^{-1}$ [*Clark et al*., 2014]. At the Wayqecha gauging station all available instantaneous discharge ($m^3 s^{-1}$) measurements ($n = 59$) over the study year were used to determine mean monthly discharge in the absence of a reliable continuous measurement of stream height. The Wayqecha Q_w record is therefore of lower precision (Table 1) and introduces more uncertainty into flux calculations than at San Pedro [*Clark et al*., 2014].

Collections of a known volume of river water (from 250 to 6400 mL) were made from the surface of the flow at the middle of the channel, in plastic bottles prerinsed with filtered river water. Larger volumes were collected during the dry season to collect sufficient SS for geochemical analyses. At both sample sites, our samples are likely to be representative of the SS load due to large-scale bed roughness which produces highly turbulent flow and mixed SS in the channel [*Lupker et al*., 2011]. The known volume of river water was filtered through 0.7 μm glass fiber filters (Whatman GF/F, 47 mm) to recover SS. Filters were dried at ~40°C within 2 days and stored in sterile petri dishes.

3.2. Geochemical Analyses

The isotopic and elemental compositions of POC were measured with an aim to assess the contribution of $POC_{biosphere}$ and POC_{petro}. Methods were identical to previous studies in this catchment [*Clark et al*., 2013], allowing direct data comparison. River SS was rinsed from the glass filter membrane using deionized water in glass beakers, and the samples were dried at 40°C [*Hilton et al*., 2010; *Clark et al*., 2013]. This procedure recovered the majority (>95%) of the sediment mass in these turbid samples but may leave behind the very finest sediment. The same procedure was carried out on precombusted quartz powder to quantify procedural blanks. The sediment mass (mg) and known filtered volume (L) were used to calculate the SS concentration (SSC; mg L^{-1}). For two SS samples from San Pedro, and four from Wayqecha, there was insufficient material (<10 mg) to process for geochemical analysis (Table S1). Samples were homogenized using an agate mortar and pestle. Inorganic carbon, such as detrital carbonate including dolomite, was removed using a 5 M HCl leach for 4 h at 75°C [*Galy et al*., 2007a; *Hilton et al*., 2008a, 2010]. Thus, all analyses reported in this study refer to acid-insoluble POC. The HCl-leach method has been shown by *Brodie et al*. [2011] to be the most robust way to return reliable organic carbon to nitrogen ratios measured in similar materials to those analyzed here. Following several deionized water rinses to remove acid salts, the suspended load samples were dried at 75°C and transferred to clean glass vials.

The weight percent organic carbon ([OC_{total}], %) and nitrogen ([N], %; used to determine the [N]/[OC_{total}] ratio) was measured using a Costech CHN elemental analyzer (EA). The results were normalized by standards and corrected for an internal and procedural blank [*Hilton et al*., 2010; *Gröcke et al*., 2011; *Clark et al*., 2013]. The stable isotope composition of POC ($\delta^{13}C_{org}$, ‰) was determined by continuous flow from the EA coupled via CONFLO-III to a Thermo-Delta-V isotope ratio mass spectrometer in the Stable Isotope Biogeochemistry Laboratory, Durham University. Values were normalized based on measured values of International Atomic Energy Agency and laboratory standards, corrected for any internal blank and procedural blank, and reported in $\delta^{13}C$ notation relative to Vienna Peedee belemnite (VPDB). The precision (2σ) and accuracy of $\delta^{13}C_{org}$ were determined using standards measured under the same analytical conditions and were both 0.1‰ [*Gröcke et al*., 2011]. Replicates of the river suspended sediment samples ($n = 21$) returned an average 2σ on $\delta^{13}C$ of ±0.1‰ and on OC_{total} of ±0.01%, and we take these as the average precision of the analyses.

A set of SS samples (9 from San Pedro and 7 from Wayqecha) were selected to measure ^{14}C activity, to expand the published measurements ($n = 21$) from the Kosñipata River [*Clark et al*., 2013]. Following the HCl decarbonation procedure detailed above, carbon in these samples was combusted, prepared to graphite, and measured by accelerator mass spectrometry at the National Ocean Sciences Accelerator Mass Spectrometry Radiocarbon Facility, Woods Hole. The data are presented here in the fraction modern (F_{mod}) terminology, corrected to −25% $\delta^{13}C$-VPDB based on measured $\delta^{13}C_{org}$ values [*Stuiver and Polach*, 1977]. The procedural blank for the filtration stage contributed <0.01% of the CO_2 used for each ^{14}C analysis, meaning that

contamination from GF/F filters was negligible within uncertainty [*Hilton et al*., 2010; *Gröcke et al*., 2011; *Clark et al*., 2013]. The inorganic carbon removal procedure did not alter the OC_{total}, $\delta^{13}C$, or F_{mod} values of standards.

3.3. Concentration-River Stage Height Relationships

Power law rating curves have been widely used to quantify solid load fluxes using continuous water discharge datasets in mountain rivers, and a growing number of studies have used them to quantify $POC_{biosphere}$ and POC_{petro} discharges in tropical [*Hilton et al*., 2011a; *Hatten et al*., 2012; *Goñi et al*., 2013; *Lloret et al*., 2013; *Smith et al*., 2013] and temperate locations [*Hilton et al*., 2011a; *Hatten et al*., 2012; *Goñi et al*., 2013; *Smith et al*., 2013]. First, the fraction of POC derived from petrogenic sources, F_{petro}, was calculated using an end-member mixing model derived for this catchment [*Clark et al*., 2013] using [N]/[OC_{total}] values (see section 4.2). The SS concentrations (SSC; $g\,m^{-3}$) were then multiplied by the [OC_{total}] and F_{petro} value to calculate the concentrations [$POC_{biosphere}$] ($g\,C\,m^{-3}$) and [POC_{petro}] ($g\,C\,m^{-3}$) in the river (Table 1). These particulate concentrations were compared to stage height (*h*; in m) to examine whether power law rating curves describe patterns in the data set [*Cohn*, 1995; *Vogel et al*., 2003; *Hilton et al*., 2008b; *Wheatcroft et al*., 2010; *Hatten et al*., 2012].

3.4. Annual SS, $POC_{biosphere}$, and POC_{petro} Discharges

At San Pedro, the 15 minute resolution stage height (*h*) measurements were used to calculate SSC, $POC_{biosphere}$, and POC_{petro} using the rating curve models. Calculated concentrations were then multiplied by Q_w derived independently from each *h* measurement [*Townsend-Small et al*., 2008; *Clark et al*., 2013; *Clark et al*., 2014]. The annual discharge of SS, $POC_{biosphere}$, and POC_{petro} were determined by summing up the 15 minute measurements for each day and then summing for each month. Yields were determined by dividing the discharge by the basin area (164.4 km^2; Table 1 and Figure 1a). Uncertainties in SSC, $POC_{biosphere}$, and POC_{petro} discharges were calculated using the standard errors of the rating curve parameters [*Turowski et al*., 2016]. Error propagation was used to quantify the uncertainty in the 15 minute solid load discharge using these values and the uncertainty in Q_w. The daily, monthly, and annual uncertainties were then calculated by additive error propagation. All annual solid load discharges were corrected for the bias introduced by fitting a linear regression to log-transformed data [*Ferguson*, 1986], as described below (see section 4.3.1).

For the Wayqecha Basin, in the absence of high temporal resolution *h* and Q_w measurements [*Townsend-Small et al*., 2008; *Clark et al*., 2013; *Clark et al*., 2014], the mean monthly SSC, $POC_{biosphere}$, and POC_{petro} were multiplied by the mean monthly Q_w to determine monthly discharge. In August there were no river measurements at the Wayqecha gauging station and linear extrapolation was carried out to determine runoff [*Clark et al*., 2014] and solid load discharge [*Clark et al*., 2013]. The fluxes were low in the dry season, including in August, so this extrapolation should not substantially affect our estimated annual yield.

3.5. Landslide Mapping

Previous work has established the decadal rates of landsliding in the valley, based on mapping from satellite imagery at an annual resolution from 1988 to 2012 [*Clark et al*., 2016]. The corresponding rates of $POC_{biosphere}$ erosion by landslides were quantified as part of this prior work. However, this previous study encompassed a larger catchment area (185 km^2), including regions downstream of the San Pedro gauging station (164.4 km^2) on the Kosñipata River (Figure 1a), and so the results are not directly comparable to those from this study (the larger area was to allow the previous work to link to forest plots further downstream). Here we use the methods and analysis explained by *Clark et al*. [2016], applied to the area of the catchment upstream of the gauging stations used in this study (Figure 1b).

4. Results

4.1. Elemental and Isotope Geochemistry

The stable isotope composition ($\delta^{13}C_{org}$), elemental composition [N]/[OC_{total}], and radiocarbon activity (F_{mod}) of POC from the SS samples collected between November 2009 and February 2011 from the Kosñipata River are consistent with the smaller, previously published data set collected over two storm events in January 2010 to February 2010 [*Clark et al*., 2013] (see Table S1). The [OC_{total}] at the San Pedro gauging station ranged from 0.48% to 6.8% with a mean of 0.99% and at the Wayqecha gauging station from 0.44% to 4.5% with a

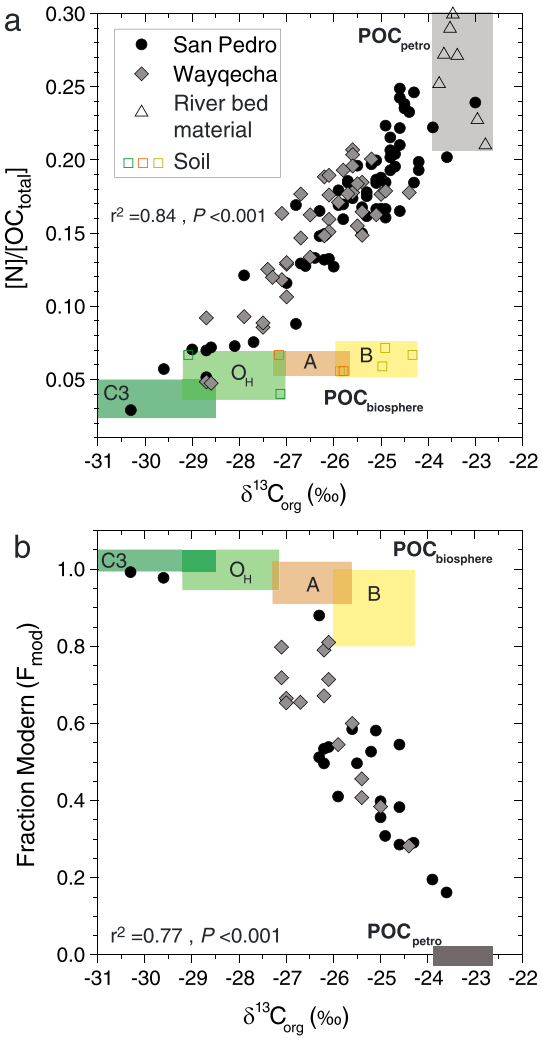

Figure 3. Elemental and isotopic compositions of POC in suspended load from the Kosñipata River from the San Pedro gauge (black circles) and from Wayqecha (grey diamonds). Published data from river bed materials (triangles) and soils (squares) from the study area are shown [*Zimmermann et al.*, 2009; *Clark et al.*, 2013]. (a) The stable isotopes of POC ($\delta^{13}C_{org}$; ‰) versus the nitrogen to organic carbon ratio ([N]/[OC_{total}]). (b) The radiocarbon activity (reported as fraction modern, F_{mod}) versus $\delta^{13}C_{org}$ (‰). The boxes show the ranges of [N]/[OC_{total}] and $\delta^{13}C_{org}$ from published sources [*Zimmermann et al.*, 2009; *Rao*, 2011] and estimates of ^{14}C activity (not measured on soils), where O_H, *A*, and *B* are the soil horizons and C3 is the C3 vegetation; all of which represent biospheric POC ($POC_{biosphere}$) sources. The grey box shows the rock-derived petrogenic POC (POC_{petro}) compositions. Analytical uncertainties are smaller than the point sizes.

mean of 1.1%. The $\delta^{13}C_{org}$ ranged from −23‰ to −30‰, and the [N]/[OCtotal] ranged from 0.03 to 0.25 (Figure 3a). The F_{mod} values ranged from 0.16 to 0.80 (Figure 3b). There were seasonal differences in $\delta^{13}C_{org}$ (‰) evident at both stations (Figure 2b). The wet season had a range in $\delta^{13}C_{org}$ values from −27‰ to −24‰. The dry season had a depleted $\delta^{13}C_{org}$ signal with values mostly between −28‰ and −29‰. The transitional seasons formed a link between the wet season and the dry season with $\delta^{13}C_{org}$ from −26‰ to −28‰ (Figure 2b).

The $\delta^{13}C_{org}$ values were linearly correlated with [N]/[OC_{total}] and F_{mod} (Figure 3). Such trends are consistent with previous work invoking a contribution to POC from rock-derived organic carbon (POC_{petro}), which is ^{14}C depleted (F_{mod}~0), is ^{13}C enriched, has high [N]/[OC_{total}] values, and is well characterized by river bed material samples (Figure 3a). The $\delta^{13}C_{org}$, [N]/[OC_{total}], and F_{mod} values can then be explained by variable addition of POC from vegetation and soil ($POC_{biosphere}$), which is ^{14}C enriched, is ^{13}C depleted, and has lower [N]/[OC_{total}] values (Figure 3). The linear trends described by $\delta^{13}C_{org}$, N/C, and F_{mod} for the suspended load (Figure 3) suggest that the majority of $POC_{biosphere}$ has a composition similar to O_H and *A* layers of the soil [*Zimmermann et al.*, 2009]. The deeper soil horizons may contribute importantly to the carbon stock on hillslopes [*Clark et al.*, 2016], particularly at lower slope angles. These deeper soils have [N]/[OC_{total}] values similar to surface soils and distinct from POC_{petro}. However, their $\delta^{13}C_{org}$ values mean that they do not appear to have been a major input to the river $POC_{biosphere}$ during our study (Figure 3). Overall, our findings concur with those from other small mountain river catchments, where POC_{petro} and $POC_{biosphere}$ are mixed during erosion and fluvial transport [*Komada et al.*, 2004; *Hilton et al.*, 2010; *Kao et al.*, 2014; *Hilton*, 2017], as well as previous work in the Kosñipata catchment [*Clark et al.*, 2013].

4.2. End-Member Mixing Analysis

Clark et al. [2013] found that the $\delta^{13}C_{org}$ and [N]/[OC_{total}] values of POC in the Kosñipata River can be quantitatively explained by a mixture of POC_{petro} from sedimentary rocks and $POC_{biosphere}$ from soil and vegetation. The additional POC samples analyzed here follow the same linear trends described in *Clark et al.* [2013], in

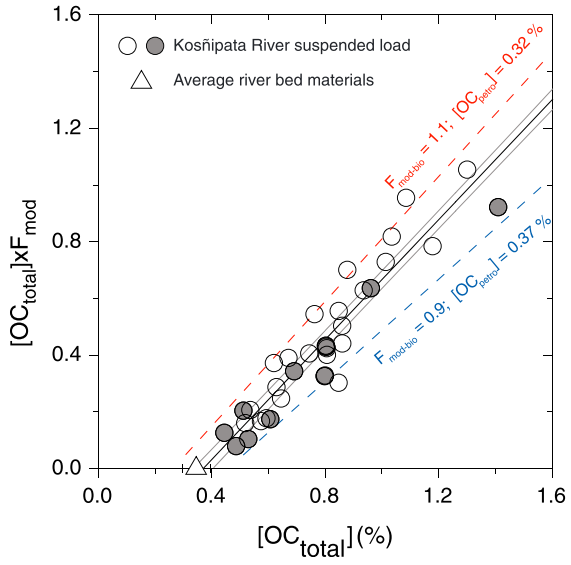

Figure 4. Organic carbon concentration [OC_{total}] versus the [OC_{total}] multiplied by the fraction modern (F_{mod}) from ^{14}C. The circles are the river samples from the Kosñipata River (the grey fills are the samples collected following the large, landslide-triggering storm event of 4 March 2010; the open circles were collected prior), and the triangle is the mean of river bed materials (assumed to have a $F_{mod} = 0$). The black line is the linear fit to the data ($r^2 = 0.99$; $p < 0.001$, $n = 35$), and grey are the 95% confidence intervals. The slope of this line corresponds to F_{mod} of the biospheric POC ($F_{mod\text{-}bio}$) of 1.05 ± 0.02 and the intercept to rock-derived organic carbon concentration, [OC_{petro}] = 0.37 ± 0.03. The red and blue lines are the mixing models based on the values of $F_{mod\text{-}bio}$ and [OC_{petro}] as shown. Analytical errors are smaller than the point sizes.

which $\delta^{13}C_{org}$ (‰) is correlated with the [N]/[OC_{total}] ratio and with F_{mod} (Figure 3). The linear trends between these ratios are consistent with the mixing hypothesis described above. Full details of how these mixing relationships were used to quantitatively partition sources can be found in *Clark et al*. [2013] (though note that $POC_{biosphere}$ and POC_{petro} are referred to as $POC_{nonfossil}$ and POC_{fossil}, respectively, in this prior paper). To briefly summarize the mixing model calculations, an end-member mixing analysis with F_{mod} from a subset of river SS samples was first used to determine the fraction of POC_{petro}, or F_{petro}, with an estimated uncertainty of 0.02. These results were then used to confirm that the [N]/[OC_{total}] ratio of the POC samples could be used to reliably quantify F_{petro} in the absence of F_{mod} measurements [*Clark et al*., 2013]. The resulting uncertainty on the calculation of F_{petro} for the Kosñipata River was found to be 0.08 to 0.14 [*Clark et al*., 2013].

We use the mixing model from *Clark et al*. [2013], the [N]/[OC_{total}] of the river POC, and the composition of end-members to quantify F_{petro} in each sample from this study. Although the radiocarbon data were used to validate our approach, the end-member mixing analysis uses [N]/[OC_{total}] to make the distinction between POC_{petro} and $POC_{biosphere}$ (Figure 3a). Therefore, the model used here cannot separate the source of $POC_{biosphere}$ between different vegetation and soil components which have relatively similar [N]/[OC_{total}] values compared to the spread of data (Figure 3a). The $POC_{biosphere}$ calculated for the measured samples (Table S1) comprised on average $0.53 \pm 0.10\%$ ($n = 66$, ±SE) of the SS at the San Pedro gauging station and $0.78 \pm 0.14\%$ ($n = 42$, ±SE) at Wayqecha. The POC_{petro} contribution was on average $0.37 \pm 0.03\%$ ($n = 66$, ±SE) and $0.34 \pm 0.02\%$ ($n = 66$, ±SE) of the SS at San Pedro and Wayqecha stations, respectively.

In addition to quantifying contributions from petrogenic versus biospheric carbon to the suspended load samples, we use the OC_{total} and F_{mod} measurements to explore the ^{14}C age of the $POC_{biosphere}$. Using previously established approaches [*Blair et al*., 2003; *Galy et al*., 2008b; *Galy and Eglinton*, 2011], we plotted [OC_{total}] against [OC_{total}] × F_{mod}. A linear trend in this space suggests that the ^{14}C activity of the biospheric POC ($F_{mod\text{-}bio}$) and the petrogenic organic carbon concentration ([OC_{petro}], %) are relatively homogeneous in the sample set [*Blair et al*., 2003; *Galy and Eglinton*, 2011]. The trend in the samples from the Kosñipata River (Figure 4) suggests that this is the case, with scatter attributable to some variability in $F_{mod\text{-}bio}$ and OC_{petro} values.

4.3. Rating Curve Models

At the San Pedro gauging station, power law rating curves describe the solid load concentrations as a function of stage height, h (Figure 5). Height (h) is used rather than Q_w [*Clark et al*., 2014] because stage height represents the measured data, simplifying uncertainty propagation. The San Pedro record includes several published data from a heavily sampled 2 week period [*Clark et al*., 2013] during which the stage height did not vary by much ($\log_{10}$[stage height] from approximately −0.15 to −0.05) when compared to the data set as a whole (Figure 5). This means that a regression model applied to the whole data set (with

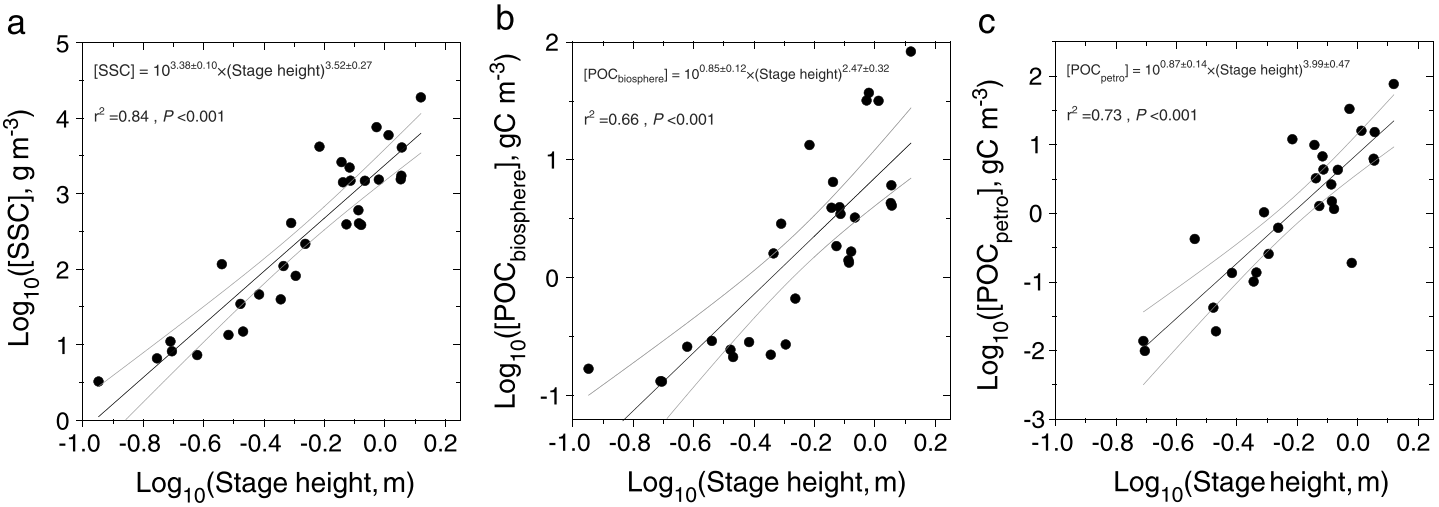

Figure 5. Relationships between river stage height and solid load constituent concentration for the Kosñipata River at San Pedro. (a) Suspended sediment concentration (SSC), (b) biospheric particulate organic carbon concentration ($POC_{biosphere}$), and (c) petrogenic POC concentration (POC_{petro}). The black lines show the linear regressions through log-transformed data and 95% confidence intervals (grey lines). Equations give the forms of rating curves used to quantify solid load discharge.

$\log_{10}$[stage height] from approximately −1.0 to +0.1) is potentially biased by these data. Therefore, we average the high-frequency measurements from this time period for each week. However, the storm peak samples were used to help constrain high-flow variability, which is difficult to sample with weekly measurements. The weekly averaging produces a data set totaling 32 data points for SSC, 30 for $POC_{biosphere}$, and 28 for POC_{petro}. Linear fits were made to log-transformed data (Figure 5), following common approaches to best describe solid load concentration over a range of flow conditions.

Measured SSC ranged from a minimum of <5 g m^{-3} to a maximum of ~19,000 g m^{-3} (Table S1). SSC was related to h and well described by a power law rating curve ($r^2 = 0.85$, $p < 0.001$; Figure 5a). Measured POC_{petro} values ranged from <0.01 g C m^{-3} up to a maximum of 77 g C m^{-3} (Table S1) and were correlated with h ($r^2 = 0.73$, $p < 0.001$; Figure 5c). POC_{petro} was closely linked with SSC as has been previously documented in mountain river-suspended load [*Blair et al.*, 2003; *Hilton et al.*, 2011a], where POC_{petro} has not been completely oxidized [*Hilton et al.*, 2014; *Hilton*, 2017]. Measured samples covered a wide range of $POC_{biosphere}$, with a minimum of ~0.1 g C m^{-3} to a maximum of 83 g C m^{-3} (Table S1). The $POC_{biosphere}$ values were correlated with h, and a power law rating curve can describe the majority of the variability ($r^2 = 0.66$, $p < 0.001$; Figure 5b). However, there was more overall scatter in the $POC_{biosphere}$-h relationship than for SSC and POC_{petro}. In all three cases, the rating curves appear to underestimate the highest measured SSC, $POC_{biosphere}$, and POC_{petro} values (Figure 5).

4.3.1. Rating Curve Bias Correction

Rating curves can be subject to known biases if fits are made to log-transformed data and then retransformed back to units of concentration or flux [*Ferguson*, 1986]. Alternatives include using nonlinear threshold rating curves [*Hilton et al.*, 2008b], linear models [*Townsend-Small et al.*, 2008; *Hilton et al.*, 2012], or flux-weighted averaging methods [*Walling and Webb*, 1981; *Ferguson*, 1987; *Dadson et al.*, 2003; *Hilton et al.*, 2012]. Here power law rating curves were used in the first instance because of the known "flashy" nature of river hydrographs in the Peruvian Andes, with storm-induced floods an important feature [*Townsend-Small et al.*, 2008; *Clark et al.*, 2013, 2014]. The observed flux-weighted mean concentrations are used as a cross-check on the rating curve estimates.

The rating curve bias is in the direction of underestimation and increases with the variance of the scatter around the underlying trend. If uncorrected, it can lead to underestimation of river constituent loads by 50% or more [*Ferguson*, 1986, 1987; *Cohn*, 1995] even when the underlying trend is of approximately power law form. If the residuals from the log-log regression have an approximately normal distribution, a simple approximate correction for the bias is to multiply C_{pred} by $\exp(2.65\, s^2)$, where C_{pred} is the concentration predicted by detransforming the log-log regression equation and s^2 is the variance of the residuals in $\log_{10}$ units [*Walling and Webb*, 1981; *Duan*, 1983; *Thomas*, 1985; *Ferguson*, 1986]. An exact correction is given by *Cohn et al.* [1989] and a nonparametric version by *Duan* [1983]. In most circumstances the three methods give similar results according to *Cohn et al.* [1989] and *Cohn* [1995], so the simplest one is used here.

For the SSC versus *h* rating curve from the Kosñipata River, the standard deviation (SD) of the linear fit to log-transformed data is 0.414, giving a (C_{true}/C_{pred}) value of 1.58. The largest bias correction is required for POC_{petro}, with a SD = 0.551 and (C_{true}/C_{pred}) = 2.23. The correction for $POC_{biosphere}$ is between these values, with SD = 0.464 and (C_{true}/C_{pred}) = 1.77. These correction values are within the range of those from the empirical data sets reported by *Ferguson* [1986]. For completeness, we report both the uncorrected and the bias-corrected solid load discharges (Table 1).

4.4. Annual SS, $POC_{biosphere}$, and POC_{petro} Discharges

4.4.1. Kosñipata River at San Pedro

The uncorrected annual SS yield based on the rating curve for the San Pedro catchment (164.4 km^2) was $2220 \pm 130\ t\ km^{-2}\ yr^{-1}$ over the water year of the study period (1 February 2010 to 31 January 2011; Table 1). Based on the annual river runoff of $2796 \pm 126\ mm\ yr^{-1}$ over the same time period [*Clark et al.*, 2014], this corresponds to an annual average SSC~$800\ g\ m^{-3}$. This value is considerably lower than both the average measured SSC = $1120 \pm 310\ g\ m^{-3}$ ($n = 68$, ±SE) and the water discharge-weighted SSC = $1560\ g\ m^{-3}$ (i.e., the flux-weighted SSC) over the sampling period. The rating curve therefore appears to underestimate the solid load concentrations measured in this river, as expected given the known bias described above (section 4.3.1). After correcting for this bias, we calculate an annual SS yield of $3500 \pm 210\ t\ km^{-2}\ yr^{-1}$ over the water year (Table 1). The corresponding annual average SSC = $1260\ g\ m^{-3}$ is in better agreement with the measurements. We therefore conclude that the bias correction produces a robust quantification of SS discharge, and by inference also $POC_{biosphere}$ and POC_{petro} yields for this catchment.

The SS yield for the Kosñipata River at San Pedro over the sampled water year (Figure 2) is larger than that reported for the Chorobamba River of the eastern Andes of Peru at ~120 to $620\ t\ km^{-2}\ yr^{-1}$ [*Townsend-Small et al.*, 2008]. This difference is expected given the steeper slopes and higher annual runoff in the Kosñipata study region. The SS yield for the water year is consistent with gauging measurements made downstream of the Kosñipata River, in the Madre de Dios River at Miraflores (124,000 km^2) from 1983 to 1990, where an estimated 71 $Mt\ yr^{-1}$ of suspended sediment were transported [*Guyot et al.*, 1996]. If this sediment is dominantly sourced from the Andes [e.g., *Gibbs*, 1967; *Meade et al.*, 1979; *Richey et al.*, 1986; *Allegre et al.*, 1996; *Dunne et al.*, 1998; *Guyot et al.*, 2005; *Filizola and Guyot*, 2009; *Martinez et al.*, 2009], which cover 35,600 km^2 (defined here as the area >550 m asl) [*Wittmann et al.*, 2009], the corresponding SS yield was ~$2000\ t\ km^{-2}\ yr^{-1}$. Based on Tropical Rainfall Measuring Mission satellite rainfall data from 1998 to 2012, 2010 was a wetter than average year [*Clark et al.*, 2014] and the SS discharge is therefore also likely to be higher than average. Therefore, the Kosñipata River SS discharge is consistent with downstream data.

The annual $POC_{biosphere}$ yield was $12.6 \pm 0.4\ t\ C\ km^{-2}\ yr^{-1}$ over the study period, when corrected for log-transformed bias using the method of *Thomas* [1985] and *Ferguson* [1986] (Table 1). Based on the measured runoff and SS yield, this corresponds to an annual average $POC_{biosphere}$ of $4.5\ g\ C\ m^{-3}$ and weight percent of $POC_{biosphere}$ in the suspended load of 0.35%. These values are consistent with the measured averages ($4.0 \pm 1.3\ g\ C\ m^{-3}$, $0.53 \pm 0.10\%$) and water-discharge-weighted averages ($5.5\ g\ C\ m^{-3}$, 0.39%), suggesting that the bias-corrected yield is a robust estimation of annual $POC_{biosphere}$ yield.

The annual POC_{petro} yield was $16.1 \pm 1.4\ t\ C\ km^{-2}\ yr^{-1}$, corrected for log-transformed bias (Table 1). This corresponds to an annual average POC_{petro} of $5.8\ g\ m^{-3}$ and weight percent of $POC_{biosphere}$ in the suspended load of 0.45%. Again, these values are consistent with the measured averages ($5.0 \pm 1.4\ g\ C\ m^{-3}$, $0.37 \pm 0.03\%$) and water-discharge-weighted averages ($6.5\ g\ C\ m^{-3}$, 0.41%).

4.4.2. Kosñipata River at Wayqecha

The annual SS yield for the Wayqecha subcatchment (48.5 km^2) was estimated to be $1270 \pm 630\ t\ km^{-2}\ yr^{-1}$ over the water year of study, based on the monthly averaging method (Table 1). The sediment yield is therefore lower in this upstream subcatchment compared to the larger catchment at San Pedro, which is consistent with the lower rates of landsliding occurring upstream of the Wayqecha gauging station [*Clark et al.*, 2016], since landslides often supply a large amount of sediment to mountain rivers [*Hovius et al.*, 2000]. The lower SS yield at Wayqecha in comparison to San Pedro is also consistent with a lower average catchment slope [*Clark et al.*, 2014; *Torres et al.*, 2015; *Clark et al.*, 2016]. The Wayqecha $POC_{biosphere}$ yield was estimated to be $5.3 \pm 2.7\ t\ C\ km^{-2}\ yr^{-1}$ and the POC_{petro} yield $3.5 \pm 1.8\ t\ C\ km^{-2}\ yr^{-1}$. These values correspond to a $\%POC_{biosphere}$ in SS of 0.46% and $\%POC_{petro}$ in SS of 0.28%.

4.5. Landslide Mobilization of $POC_{biosphere}$

We use the methods of *Clark et al*. [2016] to quantify the rate of landsliding and corresponding mobilization of $POC_{biosphere}$ from soil and vegetation. Across the catchment area upstream of San Pedro, the 25 year average landslide rate mobilized $23 \pm 4\,t\,C\,km^{-2}\,yr^{-1}$ of $POC_{biosphere}$. Of this, $4.7 \pm 0.8\,t\,C\,km^{-2}\,yr^{-1}$ was derived from vegetation (aboveground and belowground biomass) and $18 \pm 3\,t\,C\,km^{-2}\,yr^{-1}$ from soil. These yields are lower than the previously published work based on a larger catchment area (184 km^2 compared to 164.4 km^2 in this study) because landsliding rates increase downstream of a river knickpoint in the valley [*Clark et al*., 2016]. In the Wayqecha subcatchment, the 25 year average landslide rate mobilized $17 \pm 3\,t\,C\,km^{-2}\,yr^{-1}$ of $POC_{biosphere}$, $3.2 \pm 0.8\,t\,C\,km^{-2}\,yr^{-1}$ of vegetation, and $14 \pm 3\,t\,C\,km^{-2}\,yr^{-1}$ of soil.

On 4 March 2010, a large storm delivered intense precipitation [*Clark et al*., 2014] and triggered landslides which contributed importantly to the 25 year average $POC_{biosphere}$ yield [*Clark et al*., 2016]. Within the whole basin captured by the San Pedro gauge, the 2010 landslides, mostly triggered during a single storm event on 4 March 2010, mobilized $71 \pm 12\,t\,C\,km^{-2}$, of which $17 \pm 2\,t\,C\,km^{-2}$ derived from vegetation and $54 \pm 12\,t\,C\,km^{-2}$ from soil. The storm had less impact further upstream [*Clark et al*., 2014; *Clark et al*., 2016]. In the Wayqecha catchment, the 2010 landslide $POC_{biosphere}$ yield was $10 \pm 2\,t\,C\,km^{-2}$ ($1.9 \pm 0.6\,t\,C\,km^{-2}$ derived from vegetation and $8.5 \pm 2.4\,t\,C\,km^{-2}$ from soil).

5. Discussion

The lateral carbon transfer from the terrestrial biosphere to $POC_{biosphere}$ in rivers is important for carbon budgets both at the forest plot scale over annual time scales [*Berhe et al*., 2007; *Restrepo et al*., 2009; *Malhi*, 2012; *Li et al*., 2015] and at regional to global scale, over longer periods of time [*Galy et al*., 2015; *Hilton*, 2017]. Mountain rivers have been shown to have high $POC_{biosphere}$ and POC_{petro} discharges, particularly in regions which experience high runoff [*Hilton*, 2017], and distinguishing between these sources is vital to evaluate the impact of river transport on carbon budgets. Here we shed new light on the discharge of $POC_{biosphere}$ and POC_{petro} by mountain rivers, by quantifying annual yields in an Andean catchment where a suite of hydrometric, geomorphic, and ecological data sets are available [*Girardin et al*., 2010; *Malhi et al*., 2010; *Marthews et al*., 2012; *Clark et al*., 2014, 2016]. First, we assess the intraannual variability of $POC_{biosphere}$ discharge and, for the first time, directly compare annual river fluxes to estimates of landslide-mobilized $POC_{biosphere}$ inputs made over the same time window. Second, we discuss the degree to which the erosion and discharge of $POC_{biosphere}$ and POC_{petro} impact the net carbon balance of Andean forest ecosystems. Finally, we consider the fate of eroded organic carbon in the wider Amazon Basin and its role in larger-scale carbon budgets.

5.1. Fluvial Transport of $POC_{biosphere}$

The annual $POC_{biosphere}$ yields of the Kosñipata River are consistent with patterns revealed by recently published global compilations in catchments around the world [*Galy et al*., 2015; *Hilton*, 2017]. These data confirm the important role of physical erosion rate (which sets SS yield) in determining the $POC_{biosphere}$ yield (Figure 6a) [*Hilton et al*., 2012; *Galy et al*., 2015]. They also suggest that annual runoff controls the variability in $POC_{biosphere}$ yield (Figure 6b), confirming an important role of climate in regulating carbon export from the terrestrial biosphere [*Hilton*, 2017].

These global patterns arise because high catchment-average physical erosion rates are often accompanied by steep slopes in mountain environments [*Larsen et al*., 2014]. Steep slopes can enhance the erosion and supply of $POC_{biosphere}$ from soil and vegetation via two main geomorphic processes. First, bedrock landslides can clear entire tracts of mountain forest and deliver this material to the river channel network [*Hilton et al*., 2008a; *West et al*., 2011; *Clark et al*., 2016]. This process mobilizes $POC_{biosphere}$ ranging from fine-grained, mineral-associated $POC_{biosphere}$ to entire tree trunks [*Hilton et al*., 2011b; *West et al*., 2011]. Second, overland surface flow and shallow landsliding can mobilize loose material and $POC_{biosphere}$ from surface soils [*Gomi et al*., 2008], with the rate of transport depending on hillslope steepness [*Roering et al*., 2001]. Rainfall can drive both landslide activity and overland surface flow, resulting in more efficient hillslope-channel coupling and delivery of $POC_{biosphere}$ to river channels [*Hilton et al*., 2012]. We discuss these processes in more detail in the following sections.

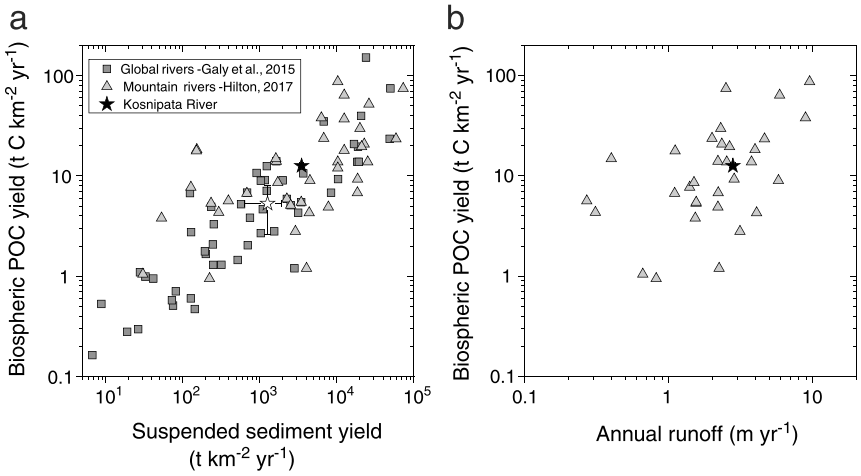

Figure 6. Biospheric POC yields for the Kosñipata River (stars) at San Pedro (black star) and Wayqecha (white star) in comparison to data from global compilations [*Galy et al*., 2015; *Hilton*, 2017] as a function of (a) suspended sediment yield and (b) annual runoff (Wayqecha not shown).

5.1.1. Intraannual Variability in $POC_{biosphere}$ Discharge

Seasonality played an important role in the erosion and discharges of SS, $POC_{biosphere}$, and POC_{petro} at the San Pedro gauging station, reflecting the geomorphic and hydrological processes operating in mountain catchments. The wet season, covering 4 months from December to March, was responsible for most of the discharges of SS (77%), $POC_{biosphere}$ (73%), and POC_{petro} (78%) (Figure 7). In the dry season (5 months from May to September), the river transported $<$5% of the annual discharge of these solid constituents.

The low Q_w values during the dry season (Figure 2) result in reduced turbulent kinetic energy, allowing fine suspended sediment and POC to settle [*Garcia and Parker*, 1991; *Hamm et al*., 2011]. The hydrological budget of this catchment shows that the majority of the river water during the dry season is sourced from delayed runoff via groundwater [*Clark et al*., 2014]. When combined with the low rainfall, this results in minimal overland flow and mass-wasting processes such as landslides, which deliver $POC_{biosphere}$ to rivers [*Hilton et al*., 2012; *Clark et al*., 2013; *Smith et al*., 2013], explaining the low $POC_{biosphere}$ discharge (Figure 7).

These geomorphic processes can also explain seasonality in the $\delta^{13}C$ and [N]/[OC_{total}] values (Figure 2b). In general, in the dry season the $\delta^{13}C$ values were more depleted at ~$-$28‰, and these samples also carry the more ^{14}C-enriched $POC_{biosphere}$ component of the POC (Figure 3b) [*Clark et al*., 2013]. With low Q_w and low rainfall, landslide activity is greatly reduced [*Clark et al*., 2016], driving less input of clastic sediment (Figure 2a) and POC_{petro}. As a result, the ratio of POC_{petro} to $POC_{biosphere}$ is lower in the dry season, explaining the bulk elemental and isotopic composition (Figures 2b and 3).

These observations contrast with previous work in the Peruvian Andes in a less steep and much less erosive catchment of the Chorobamba River [*Townsend-Small et al*., 2007; *Townsend-Small et al*., 2008]. There, in-stream photosynthesis by aquatic autotrophs is thought to be responsible for depleted $\delta^{13}C$ values during the dry season. While POC from this source could be present in the Kosñipata River during the low-turbidity dry season, we note that the dry season [N]/[OCtotal] values are 0.04–0.07, consistent with a source from vegetation and soil (Figure 3a) rather than aquatic biomass ([N]/[OCtotal] $>$0.1) [*Townsend-Small et al*., 2007].

Individual storm events and the associated rainfall-driven changes in SS load and POC transport [e.g., *Hilton et al*., 2012] influenced the mobilization and transport of material in this catchment. The largest storm in the sampling period (4–7 March 2010) had a stream runoff of 1.3 mm h^{-1} over the peak when $Q_w > 50\ m^{-3}\ s^{-1}$. This storm contributed only ~2% of the annual water discharge but was responsible for 24% of the SS yield, 14% of the $POC_{biosphere}$ yield, and 31% of the POC_{petro} yield based on the rating curve estimates. Intense runoff during such storm events can allow erosion thresholds to be surpassed at a time when fluvial transport capacity is high, explaining why these events play an important role in the erosion and transfer of soil and standing biomass to the river.

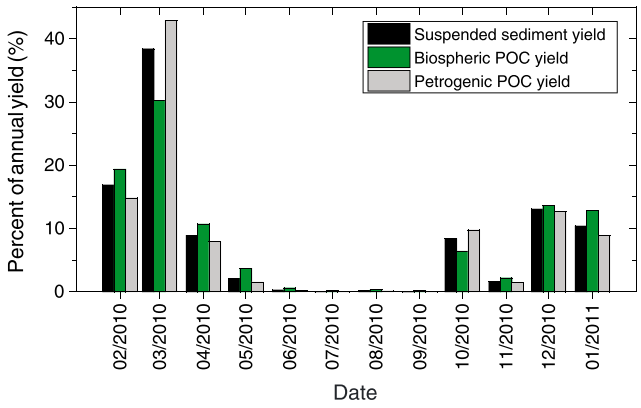

Figure 7. Annual breakdown by month of yields of suspended sediment, $POC_{biosphere}$ and POC_{petro} for the San Pedro catchment, as a percentage of the annual yield. The wet season typically represents the period from December to March.

5.1.2. Comparison Between $POC_{biosphere}$ Discharge and Landslide Inputs

Previous studies have suggested that bedrock and shallow-soil landslides can supply $POC_{biosphere}$ to mountain rivers [*Hilton et al*., 2008b, 2011b; *Hovius et al*., 2011; *West et al*., 2011; *Larsen*, 2012; *Stallard*, 2012; *Smith et al*., 2013]. In the Kosñipata Valley, landslides have been shown to play an important role in mobilizing $POC_{biosphere}$ from hillslopes [*Clark et al*., 2016]. In the San Pedro catchment, the 25 year average landslide activity mobilized $23 \pm 4\,t\,C\,km^{-2}\,yr^{-1}$ of $POC_{biosphere}$ from soil and vegetation, which is higher than the river $POC_{biosphere}$ discharge ($12.6 \pm 0.4\,t\,C\,km^{-2}\,yr^{-1}$). The difference is even larger when we compare the 2010 landslide $POC_{biosphere}$ yield of $71 \pm 12\,t\,C\,km^{-2}\,yr^{-1}$, which covers the same time period as the river gauging. The 2010 landslides were mostly triggered during the 4 March rainfall event, when an estimated $\sim 1.8\,t\,C\,km^{-2}$ of $POC_{biosphere}$ was discharged by the river-suspended load. Before now, it has not been possible to compare landslide and river $POC_{biosphere}$ discharge over the same time window for more than one storm event [*Hilton et al*., 2008b].

Two reasons for the difference between landslide-mobilized $POC_{biosphere}$ and river $POC_{biosphere}$ discharge may relate to the methods employed. Landslides can mobilize coarse materials which are not collected by most river POC sampling methods [*Turowski et al*., 2016]. The differences between the yields in the Kosñipata catchment can be explained if ~80% of the landslide-mobilized $POC_{biosphere}$ were coarse grained (i.e., coarser than sand) and thus were not sampled using our methodology. Coarse $POC_{biosphere}$ transport in rivers remains difficult to measure but can be an important component of $POC_{biosphere}$ discharge in mountain catchments [*Turowski et al*., 2013, 2016]. The second methodological issue relates to the underestimation of river $POC_{biosphere}$ discharge during the March 2010 flood, resulting from (i) underestimation of Q_w at high flow [*Clark et al*., 2014] and (ii) lacking $POC_{biosphere}$ measurements at this storm peak to validate the rating curve (Figure 2a). Both factors are likely to play some role.

Another explanation for the observed difference between estimates of landslide $POC_{biosphere}$ inputs and river $POC_{biosphere}$ discharge is process based. Some of the material mobilized by landslides can be stored within landslide deposits over decades, in analogy to clastic sediment [*Korup et al*., 2004; *Hovius et al*., 2011; *Wang et al*., 2015]. Almost all (~90%) of the landslides in the Kosñipata catchment are connected to channels that are visibly identifiable in satellite imagery [*Clark et al*., 2016]. However, not all of the landslide material may have been rapidly transported out of the catchment by the river. At high to middle elevations, landslide deposits reached small streams where the transport capacity is low. Additionally, in the lower elevations of the San Pedro catchment, alluvial sediment deposits are evident. Eroded material could remain in these deposits, contributing to a transient carbon sink, and subsequently be transferred out of the valley over an extended period of time [*Ramos Scharrón et al*., 2012]. Alternatively, carbon in landslide deposits may contribute to dissolved organic carbon after partial degradation, or be degassed from deposits, releasing CO_2 back to the atmosphere. To fully understand this component of the C erosion budget, more research needs to be done to evaluate the fate of landslide-mobilized carbon in landslide deposits, evaluating debris C stocks, CO_2 respiration, and C residence time.

5.1.3. Source and Age of $POC_{biosphere}$

In the Kosñipata River valley, the stocks of carbon in soil are large relative to lowland tropical forest [*Clark et al*., 2016]. At high elevations in the Kosñipata catchment, where temperatures are lower and hillslopes have lower slope angles [*Clark et al*., 2016], $POC_{biosphere}$ may be stored over centuries or millennia in deep *B* soil

horizons [*Rumpel and Kögel-Knabner*, 2011; *Schmidt et al*., 2011], although the ^{14}C activity of soils in this valley has not been measured (Figure 3b).

The isotopic and elemental compositions of POC in the Kosñipata River suggest that the $POC_{biosphere}$ is mostly derived from surface soil horizons (O_H and *A* layers; Figure 3a). The deeper *B* soil horizons have $\delta^{13}C_{org}$ and [N]/[OC_{total}] values [*Zimmermann et al*., 2009] which are distinct from the linear trend defined by the suspended load data (Figure 3a), indicating that the relative contribution of carbon from the deeper soil horizons to the river $POC_{biosphere}$ is small. This inference is consistent with the ^{14}C activity (Figure 3b), which suggests that the majority of samples have a $F_{mod\text{-}bio}$ value (i.e., the ^{14}C activity of the $POC_{biosphere}$) between 1.1 and 0.9 (Figure 4). These values correspond to carbon which is younger than ~850 ^{14}C years. Interestingly, the data suggest that following the 4 March 2010 storm, which triggered a large number of bedrock landslides in the catchment [*Clark et al*., 2016], the $F_{mod\text{-}bio}$ values may have been lower (between 1.0 and 0.9) than prior to the storm (Figure 4). Deep-seated landslides are capable of mobilizing deep soils and supplying this material to river channels, and the associated addition of older carbon could explain changing $F_{mod\text{-}bio}$. However, the role of aged $POC_{biosphere}$ input is hard to resolve from the bulk measurements alone. Further investigation into the age structure of POC [*Rosenheim and Galy*, 2012] and/or the ^{14}C activity of plant- and soil-derived biomarkers [*Galy and Eglinton*, 2011] could provide additional insight.

5.2. $POC_{biosphere}$ Discharge and the Carbon Budget of Andean Forest

Erosion and river transport of $POC_{biosphere}$ represents export of carbon from forest ecosystems [*Hilton et al*., 2012; *Ciais et al*., 2014; *Galy et al*., 2015]. This component of ecosystem carbon budgets is not often considered at the forest plot scale [*Iwata et al*., 2005; *Ciais et al*., 2014; *Vihermaa et al*., 2016]. In the Kosñipata River valley, the net primary production of forests (NPP—the carbon equivalent of above and belowground biomass production) is ~1000 t C km^{-2} yr^{-1} [*Malhi et al*., 2016]. The river $POC_{biosphere}$ discharge of 12.6 ± 0.4 t C km^{-2} yr^{-1} represents ~1.0% of the NPP of the forest, a similar proportion as reported elsewhere [*Hilton et al*., 2008a, 2008b; *Galy et al*., 2015].

While the $POC_{biosphere}$ flux is small compared to NPP, it is more significant when compared to the net carbon balance of the ecosystem. Net ecosystem productivity (NEP) quantifies the medium-term net carbon uptake/storage [*Marthews et al*., 2012] by accounting for heterotrophic respiration, R_h (respiration not derived from plants), where $NEP = NPP - R_h$ [*Marthews et al*., 2012]. Respiration from coarse woody material represents a significant source of uncertainty in Andean forest plots [*Girardin et al*., 2010, 2014a; *Gurdak et al*., 2014; *Huaraca Huasco et al*., 2014]. In the Kosñipata Valley, NEP has been estimated at four sites, with values ranging from $+33 \pm 52$ t C km^{-2} yr^{-1} (positive values reflecting the ecosystem being a CO_2 sink) to -172 ± 81 t C km^{-2} yr^{-1} (a CO_2 source) [*Marthews et al*., 2012; *Girardin et al*., 2014b; *Huaraca Huasco et al*., 2014].

Since these NEP values hover around zero, the export of 12.6 ± 0.4 t C km^{-2} yr^{-1} of $POC_{biosphere}$ by the Kosñipata River has the potential to tip the net carbon balance of the Andean montane forest (Figure 8). The role of erosion is more significant if we also consider the higher $POC_{biosphere}$ removal by landslides [*Clark et al*., 2016]. If $POC_{biosphere}$ in Andean Rivers such as the Kosñipata avoids respiration as it is transported downstream, and if eroded $POC_{biosphere}$ is replaced by new productivity on hillslopes, the carbon removed by rivers would strengthen the role of Andean ecosystems as a net sink of CO_2 over years to decades. The revegetation of landslide scars takes ~20–30 years [*Clark et al*., 2016], which is rapid enough to replace carbon lost to rivers, although soil carbon stocks may take longer to reestablish following landsliding [*Restrepo et al*., 2009].

Although efficient preservation of eroded $POC_{biosphere}$ could shift the Andean forest NEP to a CO_2 sink, some work suggests that Andean riverine POC is efficiently oxidized during its transit through the lowland Amazon Basin [*Quay et al*., 1992; *Hedges et al*., 2000]. If this is the case, river $POC_{biosphere}$ contributes to an increase in Andean heterotrophic respiration and reduces estimated local stand NEP by the equivalent amount (Figure 8). Some of this Andean $POC_{biosphere}$ may be many centuries old, if derived from deep soils (Figure 4 and section 5.1.3). If this older carbon and/or rock-derived POC_{petro} is also oxidized downstream [*Bouchez et al*., 2010; *Hilton et al*., 2014] (see section 5.3), and if we consider this as part of the C budget of the Andean forest plots, the impact is larger. Assuming oxidation of riverine $POC_{biosphere}$ and POC_{petro} would shift the overall NEP balance in favor of a reduced sink (or increased source) of CO_2 (Figure 8).

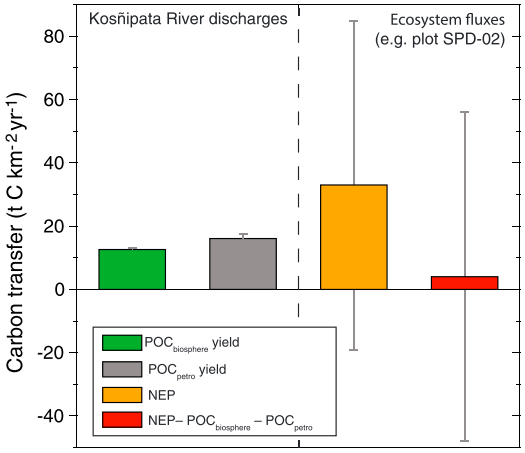

Figure 8. Kosñipata River $POC_{biosphere}$ and POC_{petro} discharges compared to net ecosystem productivity (NEP), where positive values indicate a CO_2 drawdown from the atmosphere and negative values a CO_2 source. Data from the SPD-02 plot [*Marthews et al.*, 2012] are shown for illustrative purposes. The NEP minus the $POC_{biosphere}$ and POC_{petro} discharges (i.e., assuming complete oxidation of Andean POC during riverine transit) is shown. The whiskers show the uncertainties. The red bar assumes that $POC_{biosphere}$ is oxidized. If it is instead preserved, its erosion and export would strengthen the role of Andean ecosystems as a C sink, rather than tipping the balance toward C source—emphasizing the importance of understanding the fate of eroded POC for quantifying carbon budgets.

While the fate of eroded POC from mountains reaching floodplains needs to be better constrained [*Clark et al.*, 2013; *Bouchez et al.*, 2014; *Ponton et al.*, 2014], the uncertainties on the NEP values at the plot scale are large (Figure 8) compared to the uncertainties on river discharge of $POC_{biosphere}$ and POC_{petro} [*Marthews et al.*, 2012; *Girardin et al.*, 2014b; *Huaraca Huasco et al.*, 2014]. The uncertainties on plot-scale NEP mainly relate to the challenges of measuring R_h over a representative time period, while accounting for respiration and degradation of dead coarse woody debris [*Malhi*, 2012; *Gurdak et al.*, 2014].

5.3. Andean $POC_{biosphere}$ Discharge and Contribution to the Amazon Basin Carbon Budget

The Kosñipata River drains to the Madre de Dios River (124,000 km^2), which joins the Beni River to form the Madiera River, a major tributary of the Amazon River (Figures 1c and 1d). The $POC_{biosphere}$ and POC_{petro} discharges from the Peruvian Andes have remained poorly constrained, and our measurements from a complete water year provide new insight into this component of the larger Amazon River system. If the short-term Kosñipata River $POC_{biosphere}$ yield at San Pedro is representative of the wider Andean area in the Madre de Dios Basin, where steep slopes, high rainfall, and productive forests coincide [*Killeen et al.*, 2007; *Marthews et al.*, 2012; *Asner et al.*, 2014; *Mitchard et al.*, 2014], then $POC_{biosphere}$ discharge from the Andean portion of the Madre de Dios (an area of 35,600 km^2) may reach 0.4 ± 0.2 Mt C yr^{-1}. This is 10% of the Madeira River $POC_{biosphere}$ discharge, estimated to be 4.4 Mt C yr^{-1} (Figure 9), coming from 4% of the catchment area [*Galy et al.*, 2015].

The neighboring Beni River catchment, which has a larger Andean source area, has a total $POC_{biosphere}$ discharge estimated to be 1.1 Mt C yr^{-1} [*Galy et al.*, 2015]. The corresponding $\%POC_{biosphere}$ in the suspended load of the Beni River is ~0.5%, similar to that measured in the Kosñipata River. These observations together suggest that Andean $POC_{biosphere}$ can contribute a significant flux to downstream Amazon tributaries. However, the overall Madeira $POC_{biosphere}$ discharge is much larger, which means that Andean River $POC_{biosphere}$ discharge cannot dominate the Amazon flux in the same way it is thought to do for clastic sediment (Figure 9). This observation is consistent with a substantial contribution of lowland-derived organic material to the suspended load of the larger Amazon tributaries, as inferred in the Madre de Dios from the H-isotope composition of plant-derived biomarkers [*Ponton et al.*, 2014].

The average age of biospheric POC carried by the Madeira River downstream of the Madre de Dios and Beni Rivers has been quantified as 2850 ^{14}C years [*Bouchez et al.*, 2014], much older than Andean $POC_{biosphere}$ from the Kosñipata River which is mostly $<$850 ^{14}C years (Figure 4). The older ages downstream could be a consequence of mixing older, floodplain-derived $POC_{biosphere}$ [*Lähteenoja et al.*, 2009] with younger, Andean-sourced $POC_{biosphere}$. Alternatively, Andean $POC_{biosphere}$ may be deposited and stored for hundreds to thousands of years during the exchange of sediment with the floodplain [*Aalto et al.*, 2003; *Moreira-Turcq et al.*, 2013], which represents a significant sediment flux in the rapidly meandering Beni and Madre de Dios Rivers [*Constantine et al.*, 2014]. The potential aging of Andean $POC_{biosphere}$ imposed by channel migration and floodplain storage remains to be assessed in more detail.

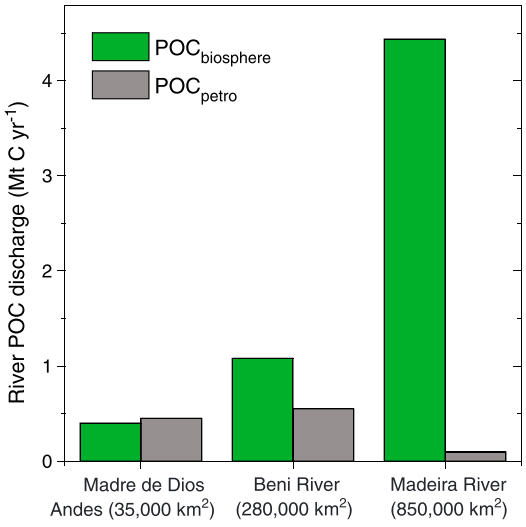

Figure 9. Estimated annual river discharge of $POC_{biosphere}$ (green) and POC_{petro} (grey) from the Madre de Dios Andes (this study) alongside published estimates from the Beni River and Madeira River [*Galy et al.*, 2015].

5.4. Andean POC_{petro} Discharge and Contribution to the Amazon Basin Carbon Budget

Erosion in the Peruvian and Bolivian Andes mobilizes POC_{petro} [*Bouchez et al.*, 2010; *Clark et al.*, 2013]. Over geological timescales, the oxidation of POC_{petro} represents a major source of CO_2 to the atmosphere alongside volcanic degassing [*Berner and Canfield*, 1989; *Derry and France-Lanord*, 1996]. The global fluxes are still uncertain [*Petsch et al.*, 2000; *Hilton et al.*, 2014] but are likely to be between 40 and 100 Mt C yr^{-1} [*Petsch*, 2014]. This CO_2 source counters geological CO_2 drawdown during the weathering of silicate minerals by carbonic acid [*Gaillardet et al.*, 1999; *Torres et al.*, 2016] and the burial of new organic matter in sediments [*Derry and France-Lanord*, 1996].

In the Kosñipata River during our study, POC_{petro} comprised ~0.45% of the SS load. Assuming that the POC_{petro} component remains coupled with the SS load [*Hilton et al.*, 2011a], the Madre de Dios River sediment flux of 71 Mt yr^{-1} [*Guyot et al.*, 1996] would equate to a POC_{petro} discharge of ~0.3 Mt C yr^{-1}. Another way to estimate the POC_{petro} discharge is using the measured annual POC_{petro} yield for the Kosñipata River (16.1 ± 1.4 t C km^{-2} yr^{-1}) over the Andean source area (35,600 km^2), giving a POC_{petro} discharge of ~0.6 Mt C yr^{-1}. For comparison, the estimate of POC_{petro} discharge in the neighboring Beni River is 0.55 Mt C yr^{-1} [*Bouchez et al.*, 2010; *Galy et al.*, 2015]. Interestingly, the ratio of $POC_{biosphere}$ to POC_{petro} discharge by these two Andean tributaries of the Madeira River appear to differ (Figure 9), which may relate to the higher proportion of POC_{petro}-bearing shales in the Madre de Dios Basin [*Carlotto Caillaux et al.*, 1996; *Clark et al.*, 2013]. The combined POC_{petro} discharge from the Beni and Madre de Dios Rivers is larger than that exported to the Bay of Bengal by the Ganges-Brahmaputra Rivers [*Galy et al.*, 2007b; *Galy et al.*, 2008a].

At the outlet of the Madeira River, *Bouchez et al.* [2010] estimate that 0.02% of the SS is POC_{petro}, with a corresponding POC_{petro} discharge of 0.1 Mt C yr^{-1} [*Galy et al.*, 2015]. The Madeira River's sediment load comprises sediments from the Madre de Dios, Beni, and Mamoré Rivers. Combining the estimates of the Andean POC_{petro} discharge from the Beni and Madre de Dios gives ~0.9–1.1 Mt C yr^{-1}, and therefore, there is a marked discrepancy of ~1 Mt C yr^{-1} between the Andean POC_{petro} input and Madeira River output, without even accounting from any additional contribution from the Mamoré (Figure 9). POC_{petro} may be preferentially buried in the lowland floodplain during overbank deposition [*Dunne et al.*, 1998; *Aalto et al.*, 2003]. Alternatively, POC_{petro} may have been oxidized during floodplain transit [*Bouchez et al.*, 2010]. Supporting this interpretation, ^{14}C measurements of CO_2 degassing from the Tambopata River, a small tributary of the Madre de Dios with Andean headwaters, suggest a role of geological sources [*Vihermaa et al.*, 2014]. The total difference between the Madeira River output and its Andean sources suggest a potential release of ~1 Mt C yr^{-1} of geological CO_2 to the atmosphere [*Bouchez et al.*, 2010]. This flux is larger than the CO_2 drawdown via silicate weathering in the Madeira Basin, of ~0.8 Mt C yr^{-1} [*Gaillardet et al.*, 1999], providing a strong impetus to better constrain the flux and fate of POC_{petro} in the Amazon Basin and its contribution to CO_2 degassing.

6. Conclusions

We quantify the SS, $POC_{biosphere}$, and POC_{petro} yields for the Kosñipata River, in the Peruvian Andes (Figure 1), where we draw from parallel data sets on hydrology, ecology, and rates of geomorphic processes to understand these yields and to assess their impact on local to regional carbon cycles. We use carbon isotopes (^{14}C,

^{13}C, and ^{12}C) and [N]/[OC_{total}] ratios to distinguish POC from sedimentary rocks (POC_{petro}) and POC from the terrestrial biosphere ($POC_{biosphere}$) (Figure 3). At the San Pedro gauging station (164.4 km^2), the SSC, $POC_{biosphere}$, and POC_{petro} (instantaneous concentrations in the river) are well described by power law rating curves as a function of river stage height. These rating curves are applied to a continuous water stage record to quantify daily, monthly, and annual yields. We correct for the known underestimation of river loads due to statistical bias in the rating curve method, correcting yields by a factor of 1.58 for SS, 1.77 for $POC_{biosphere}$, and 2.23 for POC_{petro}.

Over the water year of study (1 February 2010 to 31 January 2011), we calculate a SS yield of 3500 ± 210 t km^{-2} yr^{-1}, >15 times the Amazon Basin average. The bias-corrected rating curve estimates return a $POC_{biosphere}$ yield of 12.6 ± 0.4 t C km^{-2} yr^{-1} and a POC_{petro} yield of 16.1 ± 1.4 t C km^{-2} yr^{-1}. The yields are lower at the upstream Wayqecha gauging station, where catchment average slope, rainfall, and landslide rates are lower (Table 1 and Figure 1b). The erosional transfers of $POC_{biosphere}$ confirm the global importance of SS yield and annual runoff for setting carbon export from the biosphere (Figure 6). The $POC_{biosphere}$ discharge is large enough that it can play an important role in the NEP of Andean forest. If one also considers eroded POC_{petro}, the river POC is even more significant. For example, if river $POC_{biosphere}$ and POC_{petro} were efficiently oxidized following export from the Andes, the NEP at Andean sites would be reduced to $<+4 \pm 52$ t C km^{-2} yr^{-1} (Figure 8). However, the river POC discharges are within the uncertainty on the NEP estimates.

We use our measurements to provide a first estimate of Andean $POC_{biosphere}$ discharge delivered to the Madre de Dios River (Andean area = 35,600 km^2) of 0.4 ± 0.2 Mt C yr^{-1}, which is ~10% of the Madeira River $POC_{biosphere}$ discharge, from 4% of the catchment area (Figure 9). Consequently, while Andean erosion is thought to supply the vast majority of SS to the lowland Amazon, lowland sources must also be important for riverine $POC_{biosphere}$. In contrast, the estimated Andean POC_{petro} discharge delivered to the Madre de Dios River (0.3–0.6 Mt C yr^{-1}) is 300% of the Madeira River POC_{petro} discharge. Net oxidation of Andean POC_{petro} during lowland transit may release significant amounts of CO_2 to the atmosphere, while transient storage of $POC_{biosphere}$ and its contribution to oceanic POC export represent an important CO_2 sink. The fate of Andean $POC_{biosphere}$ and POC_{petro} in the lowland rivers of the Amazon basin needs to be better constrained in order to fully quantify the impact of erosion and lateral carbon fluxes on the CO_2 budget of the Amazon ecosystem.

Acknowledgments

This paper is a product of the Andes Biodiversity and Ecosystems Research Group (ABERG). K.E.C. was funded by the Natural Sciences and Engineering Research Council of Canada (362718-2008 PGS-D3) and Clarendon Fund PhD scholarships. R.G.H. was supported by a NERC New Investigator Grant (NE/I001719/1) and a European Research Council Starting Grant ROC-CO_2 (678779). A.J.W. was supported to work in the Kosñipata catchment by NSF-EAR 1227192 and 1455352. Y.M. is supported by the Jackson Foundation and a European Research Council advanced investigator grant GEM-TRAITS (321131) under the European Union's Seventh Framework Programme (FP7/2007–2013). We thank ACCA Peru (Wayqecha) and Inkaterra (San Pedro) for the field support and L.V. Morales, R.J. Abarca Martínez, M.H. Yucra Hurtado, R. Paja Yurca, J.A. Gibaja Lopez, I. Cuba Torres, J. Huamán Ovalle, A. Alfaro-Tapia, R. Butrón Loayza, J. Farfan Flores, D. Oviedo Licona, and D. Ocampo for the field assistance. The Carnegie Airborne Observatory is made possible by the Avatar Alliance Foundation, Grantham Foundation for the Protection of the Environment, John D. and Catherine T. MacArthur Foundation, Gordon and Betty Moore Foundation, W.M. Keck Foundation, Margaret A. Cargill Foundation, Mary Anne Nyburg Baker and G. Leonard Baker Jr., and William R. Hearst III. We thank D. Knapp, T. Kennedy-Bowdoin, C. Anderson, and R. Tupayachi for the CAO data collection and analysis. We thank S. Waldron, S. Dadson, S. Lane, S. Feakins, and C. Ponton for their helpful discussions and comments prior to submission and V. Galy for suggesting the radiocarbon analysis of the poststorm samples. We thank Editor M. Goni and two anonymous reviewers for their comments on the paper which helped improve the manuscript. Data not included in the tables in this paper or its supporting information are available in association with cited publications, including discharge and stage height records [*Clark et al.*, 2014; http://dx.doi.org/10.4211/hs.5f432a520370472683b543d493f136d1] and the Kosñipata valley landslide inventory [*Clark et al.*, 2016; http://dx.doi.org/10.4211/hs.90487bcf16e44c62a677ae33ef95e968].

References

Aalto, R., L. Maurice-Bourgoin, T. Dunne, D. R. Montgomery, C. A. Nittrouer, and J. L. Guyot (2003), Episodic sediment accumulation on Amazonian flood plains influenced by El Niño/Southern Oscillation, *Nature*, *425*(6957), 493–497, doi:10.1038/nature02002.

Allegre, C. J., B. Dupre, P. Negrel, and J. Gaillardet (1996), Sr-Nd-Pb isotope systematics in Amazon and Congo River systems: Constraints about erosion processes, *Chem. Geol.*, *131*(1–4), 93–112, doi:10.1016/0009-2541(96)00028-9.

Asner, G. P., C. B. Anderson, R. E. Martin, D. E. Knapp, R. Tupayachi, F. Sinca, and Y. Malhi (2014), Landscape-scale changes in forest structure and functional traits along an Andes-to-Amazon elevation gradient, *Biogeosciences*, *11*(3), 843–856, doi:10.5194/bg-11-843-2014.

Aufdenkampe, A. K., E. Mayorga, J. I. Hedges, C. Llerena, P. D. Quay, J. Gudeman, A. V. Krusche, and J. E. Richey (2007), Organic matter in the Peruvian headwaters of the Amazon: Compositional evolution from the Andes to the lowland Amazon mainstem, *Org. Geochem.*, *38*(3), 337–364, doi:10.1016/j.orggeochem.2006.06.003.

Berhe, A. A., J. Harte, J. W. Harden, and M. S. Torn (2007), The significance of the erosion-induced terrestrial carbon sink, *BioScience*, *57*(4), 337–346, doi:10.1641/b570408.

Berner, R. A. (1982), Burial of organic carbon and pyrite sulfur in the modern ocean: Its geochemical and environmental significance, *Am. J. Sci.*, *282*(4), 451–473.

Berner, R. A., and D. E. Canfield (1989), A new model for atmospheric oxygen over Phanerozoic time, *Am. J. Sci.*, *289*(4), 333–361, doi:10.2475/ajs.289.4.333.

Blair, N. E., and R. C. Aller (2012), The fate of terrestrial organic carbon in the marine environment, *Annu. Rev. Mar. Sci.*, *4*, 401–423, doi:10.1146/annurev-marine-120709-142717.

Blair, N. E., E. L. Leithold, S. T. Ford, K. A. Peeler, J. C. Holmes, and D. W. Perkey (2003), The persistence of memory: The fate of ancient sedimentary organic carbon in a modern sedimentary system, *Geochim. Cosmochim. Acta*, *67*(1), 63–73, doi:10.1016/s0016-7037(02)01043-8.

Blodgett, T. A., and B. L. Isacks (2007), Landslide erosion rate in the eastern cordillera of northern Bolivia, *Earth Interact.*, *11*, 1–30, doi:10.1175/2007EI222.1.

Bouchez, J., O. Beyssac, V. Galy, J. Gaillardet, C. France-Lanord, L. Maurice, and P. Moreira-Turcq (2010), Oxidation of petrogenic organic carbon in the Amazon floodplain as a source of atmospheric CO_2, *Geology*, *38*(3), 255–258, doi:10.1130/g30608.1.

Bouchez, J., V. Galy, R. G. Hilton, J. Gaillardet, P. Moreira-Turcq, M. A. Pérez, C. France-Lanord, and L. Maurice (2014), Source, transport and fluxes of Amazon River particulate organic carbon: Insights from river sediment depth-profiles, *Geochim. Cosmochim. Acta*, *133*, 280–298, doi:10.1016/j.gca.2014.02.032.

Brodie, C. R., M. J. Leng, J. S. L. Casford, C. P. Kendrick, J. M. Lloyd, Z. Yongqiang, and M. I. Bird (2011), Evidence for bias in C and N concentrations and $\delta^{13}C$ composition of terrestrial and aquatic organic materials due to pre-analysis acid preparation methods, *Chem. Geol.*, *282*(3), 67–83, doi:10.1016/j.chemgeo.2011.01.007.

Carlotto Caillaux, V. S., G. Rodriguez, W. Fernando, C. Roque, J. Dionicio, and R. Chávez (1996), *Geología de los cuadrángulos de Urubamba y Calca*, Instituto Geológica Nacional, Lima, Peru. [Available at http://www.ingemmet.gob.pe/publicaciones/serie_a/mapas/27-s.htm.]

Ciais, P., A. Dolman, A. Bombelli, R. Duren, A. Peregon, P. Rayner, C. Miller, N. Gobron, G. Kinderman, and G. Marland (2014), Current systematic carbon-cycle observations and the need for implementing a policy-relevant carbon observing system, *Biogeosciences*, *11*, 3547–3602, doi:10.5194/bg-11-3547-2014.

Clark, K. E., R. G. Hilton, A. J. West, Y. Malhi, D. R. Gröcke, C. L. Bryant, P. L. Ascough, A. Robles Caceres, and M. New (2013), New views on "old" carbon in the Amazon River: Insight from the source of organic carbon eroded from the Peruvian Andes, *Geochem. Geophys. Geosyst.*, *14*, 1644–1659, doi:10.1002/ggge.20122.

Clark, K. E., M. A. Torres, A. J. West, R. G. Hilton, M. New, A. B. Horwath, J. B. Fisher, J. M. Rapp, A. Robles Caceres, and Y. Malhi (2014), The hydrological regime of a forested tropical Andean catchment, *Hydrol. Earth Syst. Sci.*, *18*, 5377–5397, doi:10.5194/hess-18-5377-2014.

Clark, K. E., et al. (2016), Storm-triggered landslides in the Peruvian Andes and implications for topography, carbon cycles, and biodiversity, *Earth Surf. Dyn.*, *4*, 47–70, doi:10.5194/esurf-4-47-2016.

Cohn, T. A. (1995), Recent advances in statistical methods for the estimation of sediment and nutrient transport in rivers, *Rev. Geophys.*, *33*, 1117–1123, doi:10.1029/95RG00292.

Cohn, T. A., L. L. Delong, E. J. Gilroy, R. M. Hirsch, and D. K. Wells (1989), Estimating constituent loads, *Water Resour. Res.*, *25*, 937–942, doi:10.1029/WR025i005p00937.

Constantine, J. A., T. Dunne, J. Ahmed, C. Legleiter, and E. D. Lazarus (2014), Sediment supply as a driver of river meandering and floodplain evolution in the Amazon Basin, *Nat. Geosci.*, *7*(12), 899–903, doi:10.1038/ngeo2282.

Dadson, S. J., et al. (2003), Links between erosion, runoff variability and seismicity in the Taiwan orogen, *Nature*, *426*(6967), 648–651, doi:10.1038/nature02150.

Derry, L. A., and C. France-Lanord (1996), Neogene growth of the sedimentary organic carbon reservoir, *Paleoceanography*, *11*, 267–275, doi:10.1029/95PA03839.

Dixon, R. K., S. Brown, R. Houghton, A. Solomon, M. Trexler, and J. Wisniewski (1994), Carbon pools and flux of global forest ecosystems, *Science*, *263*(5144), 185–189.

Duan, N. (1983), Smearing estimate: A nonparametric retransformation method, *J. Am. Stat. Assoc.*, *78*(383), 605–610, doi:10.1080/01621459.1983.10478017.

Dunne, T., L. A. K. Mertes, R. H. Meade, J. E. Richey, and B. R. Forsberg (1998), Exchanges of sediment between the flood plain and channel of the Amazon River in Brazil, *Geol. Soc. Am. Bull.*, *110*(4), 450–467.

Eva, H. D., et al. (2005), A proposal for defining the geographical boundaries of Amazonia Synthesis of the results from an Expert Consultation Workshop organised by the European Commission in collaboration with the Amazon Cooperation Treaty Organization-JRC Ispra, European Communities, Luxembourg, 7–8 June.

Feng, X., et al. (2016), Source to sink: Evolution of lignin composition in the Madre de Dios River system with connection to the Amazon basin and offshore, *J. Geophys. Res. Biogeosci.*, *121*, 1316–1338, doi:10.1002/2016JG003323.

Ferguson, R. I. (1986), River loads underestimated by rating curves, *Water Resour. Res.*, *22*, 74–76, doi:10.1029/WR022i001p00074.

Ferguson, R. I. (1987), Accuracy and precision of methods for estimating river loads, *Earth Surf. Processes Landforms*, *12*(1), 95–104, doi:10.1002/esp.3290120111.

Filizola, N., and J. L. Guyot (2009), Suspended sediment yields in the Amazon basin: An assessment using the Brazilian national data set, *Hydrol. Processes*, *23*(22), 3207–3215, doi:10.1002/hyp.7394.

France-Lanord, C., and L. A. Derry (1997), Organic carbon burial forcing of the carbon cycle from Himalayan erosion, *Nature*, *390*(6655), 65–67.

Gaillardet, J., B. Dupré, P. Louvat, and C. J. Allègre (1999), Global silicate weathering and CO_2 consumption rates deduced from the chemistry of large rivers, *Chem. Geol.*, *159*(1–4), 3–30, doi:10.1016/S0009-2541(99)00031-5.

Galy, V., and T. Eglinton (2011), Protracted storage of biospheric carbon in the Ganges-Brahmaputra basin, *Nat. Geosci.*, *4*(12), 843–847, doi:10.1038/ngeo1293.

Galy, V., J. Bouchez, and C. France-Lanord (2007a), Determination of total organic carbon content and delta C-13 in carbonate-rich detrital sediments, *Geostand. Geoanal. Res.*, *31*(3), 199–207, doi:10.1111/j.1751-908X.2007.00864.x.

Galy, V., C. France-Lanord, O. Beyssac, P. Faure, H. Kudrass, and F. Palhol (2007b), Efficient organic carbon burial in the Bengal fan sustained by the Himalayan erosional system, *Nature*, *450*(7168), 204–207, doi:10.1038/nature06273.

Galy, V., O. Beyssac, C. France-Lanord, and T. Eglinton (2008a), Recycling of graphite during Himalayan erosion: A geological stabilization of carbon in the crust, *Science*, *322*(5903), 943–945, doi:10.1126/science.1161408.

Galy, V., C. France-Lanord, and B. Lartiges (2008b), Loading and fate of particulate organic carbon from the Himalaya to the Ganga-Brahmaputra delta, *Geochim. Cosmochim. Acta*, *72*(7), 1767–1787, doi:10.1016/j.gca.2008.01.027.

Galy, V., B. Peucker-Ehrenbrink, and T. Eglinton (2015), Global carbon export from the terrestrial biosphere controlled by erosion, *Nature*, *521*(7551), 204–207, doi:10.1038/nature14400.

Garcia, M., and G. Parker (1991), Entrainment of bed sediment into suspension, *J. Hydraul. Eng.*, *117*(4), 414–435, doi:10.1061/(ASCE)0733-9429(1991)117:4(414).

Gibbs, R. J. (1967), Amazon River—Environmental factors that control its dissolved and suspended load, *Science*, *156*(3783), 1734–1737.

Girardin, C. A. J., et al. (2010), Net primary productivity allocation and cycling of carbon along a tropical forest elevational transect in the Peruvian Andes, *Global Change Biol.*, *16*(12), 3176–3192, doi:10.1111/j.1365-2486.2010.02235.x.

Girardin, C. A. J., et al. (2014a), Seasonality of above-ground net primary productivity along an Andean altitudinal transect in Peru, *J. Trop. Ecol.*, *30*(06), 503–519, doi:10.1017/S0266467414000443.

Girardin, C. A. J., et al. (2014b), Productivity and carbon allocation in a tropical montane cloud forest of the Peruvian Andes, *Plant Ecol. Divers.*, *7*(1–2), 107–123, doi:10.1080/17550874.2013.820222.

Gomi, T., R. C. Sidle, M. Ueno, S. Miyata, and K. Kosugi (2008), Characteristics of overland flow generation on steep forested hillslopes of central Japan, *J. Hydrol.*, *361*(3), 275–290, doi:10.1029/2007WR005894.

Goñi, M. A., J. A. Hatten, R. A. Wheatcroft, and J. C. Borgeld (2013), Particulate organic matter export by two contrasting small mountainous rivers from the Pacific Northwest, USA, *J. Geophys. Res. Biogeosci.*, *118*, 112–134, doi:10.1002/jgrg.20024.

Gregory-Wodzicki, K. M. (2000), Uplift history of the central and Northern Andes: A review, *Geol. Soc. Am. Bull.*, *112*(7), 1091–1105, doi:10.1130/0016-7606(2000)112 < 1091:UHOTCA > 2.0.CO;2.

Gröcke, D. R., R. S. Hori, J. Trabucho-Alexandre, D. B. Kemp, and L. Schwark (2011), An open ocean record of the Toarcian oceanic anoxic event, *Solid Earth*, *2*, 245–257, doi:10.5194/se-2-245-2011.

Gurdak, D. J., et al. (2014), Assessing above-ground woody debris dynamics along a gradient of elevation in Amazonian cloud forests in Peru: Balancing above-ground inputs and respiration outputs, *Plant Ecol. Divers.*, *7*(1–2), 143–160, doi:10.1080/17550874.2013.818073.

Guyot, J. L., N. Fillzola, J. Quintanilla, and J. Cortez (1996), Dissolved solids and suspended sediment yields in the Rio Madeira basin, from the Bolivian Andes to the Amazon, *IAHS Publ.*, *236*, 55–64.

Guyot, J. L., N. Filizola, and A. Laraque (2005), The suspended sediment flux of the River Amazon at Obidos, Brazil, 1995–2003, in *Sediment Budgets 1*, edited by D. E. Walling and A. J. Horowitz, pp. 347–354 , International Association of Hydrological Sciences, Wallingford, UK.
Hamm, N. T., W. B. Dade, and C. E. Renshaw (2011), Fine particle deposition to porous beds, *Water Resour. Res.*, *47*, W11508, doi:10.1029/2010WR010295.
Hatten, J. A., M. A. Goñi, and R. A. Wheatcroft (2012), Chemical characteristics of particulate organic matter from a small, mountainous river system in the Oregon Coast Range, USA, *Biogeochemistry*, 1–24, doi:10.1007/s10533-010-9529-z.
Hedges, J. I., et al. (2000), Organic matter in Bolivian tributaries of the Amazon River: A comparison to the lower mainstream, *Limnol. Oceanogr.*, *45*(7), 1449–1466.
Hicks, D. M., B. Gomez, and N. A. Trustrum (2000), Erosion thresholds and suspended sediment yields, Waipaoa River Basin, New Zealand, *Water Resour. Res.*, *36*, 1129–1142, doi:10.1029/1999WR900340.
Hilton, R. G. (2017), Climate regulates the erosional carbon export from the terrestrial biosphere, *Geomorphology*, *277*, 118–132, doi:10.1016/j.geomorph.2016.03.028.
Hilton, R. G., A. Galy, and N. Hovius (2008a), Riverine particulate organic carbon from an active mountain belt: Importance of landslides, *Global Biogeochem. Cycles*, *22*, BG1017, doi:10.1029/2006GB002905.
Hilton, R. G., A. Galy, N. Hovius, M.-C. Chen, M.-J. Horng, and H. Chen (2008b), Tropical-cyclone-driven erosion of the terrestrial biosphere from mountains, *Nat. Geosci.*, *1*(11), 759–762, doi:10.1038/ngeo333.
Hilton, R. G., A. Galy, N. Hovius, M.-J. Horng, and H. Chen (2010), The isotopic composition of particulate organic carbon in mountain rivers of Taiwan, *Geochim. Cosmochim. Acta*, *74*(11), 3164–3181, doi:10.1016/j.gca.2010.03.004.
Hilton, R. G., A. Galy, N. Hovius, M.-J. Horng, and H. Chen (2011a), Efficient transport of fossil organic carbon to the ocean by steep mountain rivers: An orogenic carbon sequestration mechanism, *Geology*, *39*(1), 71–74, doi:10.1130/g31352.1.
Hilton, R. G., P. Meunier, N. Hovius, P. J. Bellingham, and A. Galy (2011b), Landslide impact on organic carbon cycling in a temperate montane forest, *Earth Surf. Processes Landforms*, *36*(12), 1670–1679, doi:10.1002/esp.2191.
Hilton, R. G., A. Galy, N. Hovius, S.-J. Kao, M.-J. Horng, and H. Chen (2012), Climatic and geomorphic controls on the erosion of terrestrial biomass from subtropical mountain forest, *Global Biogeochem. Cycles*, *26*, GB3014, doi:10.1029/2012gb004314.
Hilton, R. G., J. Gaillardet, D. Calmels, and J.-L. Birck (2014), Geological respiration of a mountain belt revealed by the trace element rhenium, *Earth Planet. Sci. Lett.*, *403*, 27–36, doi:10.1016/j.epsl.2014.06.021.
Hilton, R. G., V. Galy, J. Gaillardet, M. Dellinger, C. Bryant, M. O'Regan, D. R. Grocke, H. Coxall, J. Bouchez, and D. Calmels (2015), Erosion of organic carbon in the Arctic as a geological carbon dioxide sink, *Nature*, *524*(7563), 84–87, doi:10.1038/nature14653.
Houghton, R. A. (2005), Aboveground forest biomass and the global carbon balance, *Global Change Biol.*, *11*(6), 945–958, doi:10.1111/j.1365-2486.2005.00955.x.
Hovius, N., C. P. Stark, H. T. Chu, and J. C. Lin (2000), Supply and removal of sediment in a landslide-dominated mountain belt: Central Range, Taiwan, *J. Geol.*, *108*(1), 73–89, doi:10.1086/314387.
Hovius, N., A. Galy, R. G. Hilton, R. Sparkes, J. Smith, K. Shuh-Ji, C. Hongey, L. In-Tian, and A. J. West (2011), Erosion-driven drawdown of atmospheric carbon dioxide: The organic pathway, *Appl. Geochem.*, *26*, S285–S287, doi:10.1016/j.apgeochem.2011.03.082.
Huaraca Huasco, W., et al. (2014), Seasonal production, allocation and cycling of carbon in two mid-elevation tropical montane forest plots in the Peruvian Andes, *Plant Ecol. Divers.*, *1–2*(1–2), 125–142, doi:10.1080/17550874.2013.819042.
INGEMMET (2013), GEOCATMIN—Geologia integrada por proyectos regionales, Lima, Peru.
Iwata, H., Y. Malhi, and C. von Randow (2005), Gap-filling measurements of carbon dioxide storage in tropical rainforest canopy airspace, *Agr. Forest Meteorol.*, *132*(3–4), 305–314, doi:10.1016/j.agrformet.2005.08.005.
Kao, S. J., and J. D. Milliman (2008), Water and sediment discharge from small mountainous rivers, Taiwan: The roles of lithology, episodic events, and human activities, *J. Geol.*, *116*(5), 431–448, doi:10.1086/590921.
Kao, S. J., and K. K. Liu (1997), Fluxes of dissolved and nonfossil particulate organic carbon from an Oceania small river (Lanyang Hsi) in Taiwan, *Biogeochemistry*, *39*(3), 255–269.
Kao, S. J., et al. (2014), Preservation of terrestrial organic carbon in marine sediments offshore Taiwan: Mountain building and atmospheric carbon dioxide sequestration, *Earth Surf. Dyn.*, *2*(1), 127–139, doi:10.5194/esurf-2-127-2014.
Killeen, T. J., M. Douglas, T. Consiglio, P. M. Jørgensen, and J. Mejia (2007), Dry spots and wet spots in the Andean hotspot, *J. Biogeogr.*, *34*(8), 1357–1373, doi:10.1111/j.1365-2699.2006.01682.x.
Komada, T., E. R. M. Druffel, and S. E. Trumbore (2004), Oceanic export of relict carbon by small mountainous rivers, *Geophys. Res. Lett.*, *31*, L07504, doi:10.1029/2004gl019512.
Korup, O., M. J. McSaveney, and T. R. H. Davies (2004), Sediment generation and delivery from large historic landslides in the Southern Alps, New Zealand, *Geomorphology*, *61*(1–2), 189–207, doi:10.1016/j.geomorph.2004.01.001.
Lähteenoja, O., K. Ruokolainen, L. Schulman, and M. Oinonen (2009), Amazonian peatlands: An ignored C sink and potential source, *Global Change Biol.*, *15*(9), 2311–2320, doi:10.1111/j.1365-2486.2009.01920.x.
Larsen, I. J., D. R. Montgomery, and H. M. Greenberg (2014), The contribution of mountains to global denudation, *Geology*, *42*, 527–530, doi:10.1130/G35136.1.
Larsen, M. C. (2012), Landslides and sediment budgets in four watersheds in eastern Puerto Rico: Chapter F, in *Water Quality and Landscape Processes of Four Watersheds in Eastern Puerto Rico*, edited by S. F. Murphy and R. F. Stallard, pp. 153–178, U.S. Geol. Surv. Prof. Pap., *1789*.
Lehner, B., K. Verdin, and A. Jarvis (2008), New global hydrography derived from spaceborne elevation data, *Eos Trans. AGU*, *89*(10), 93–94, doi:10.1029/2008EO100001.
Li, Y., T. A. Quine, H. Q. Yu, G. Govers, J. Six, D. Z. Gong, Z. Wang, Y. Z. Zhang, and K. Van Oost (2015), Sustained high magnitude erosional forcing generates an organic carbon sink: Test and implications in the Loess Plateau, China, *Earth Planet. Sci. Lett.*, *411*, 281–289, doi:10.1016/j.epsl.2014.11.036.
Lloret, E., C. Dessert, L. Pastor, E. Lajeunesse, O. Crispi, J. Gaillardet, and M. F. Benedetti (2013), Dynamic of particulate and dissolved organic carbon in small volcanic mountainous tropical watersheds, *Chem. Geol.*, *351*, 229–244, doi:10.1016/j.chemgeo.2013.05.023.
Lupker, M., C. France-Lanord, J. Lavé, J. Bouchez, V. Galy, F. Métivier, J. Gaillardet, B. Lartiges, and J.-L. Mugnier (2011), A Rouse-based method to integrate the chemical composition of river sediments: Application to the Ganga basin, *J. Geophys. Res.*, *116*, F04012, doi:10.1029/2010jf001947.
Lyons, W. B., C. A. Nezat, A. E. Carey, and D. M. Hicks (2002), Organic carbon fluxes to the ocean from high-standing islands, *Geology*, *30*(5), 443–446, doi:10.1130/0091-7613(2002)030 < 0443:ocftto > 2.0.co;2.
Malhi, Y. (2010), The carbon balance of tropical forest regions, 1990–2005, *Curr. Opin. Environ. Sust.*, *2*(4), 237–244, doi:10.1016/j.cosust.2010.08.002.
Malhi, Y. (2012), The productivity, metabolism and carbon cycle of tropical forest vegetation, *J. Ecol.*, *100*(1), 65–75, doi:10.1111/j.1365-2745.2011.01916.x.

Malhi, Y., M. Silman, N. Salinas, M. Bush, P. Meir, and S. Saatchi (2010), Introduction: Elevation gradients in the tropics: Laboratories for ecosystem ecology and global change research, *Global Change Biol.*, *16*(12), 3171–3175, doi:10.1111/j.1365-2486.2010.02323.x.

Malhi, Y., et al. (2016), The variation of productivity and its allocation along a tropical elevation gradient: A whole carbon budget perspective, *New Phytol.*, 1–14, doi:10.1111/nph.14189.

Marengo, J. A., W. R. Soares, C. Saulo, and M. Nicolini (2004), Climatology of the low-level jet east of the Andes as derived from the NCEP-NCAR reanalyses: Characteristics and temporal variability, *J. Clim.*, *17*(12), 2261–2280, doi:10.1175/1520-0442(2004)017 < 2261:COTLJE > 2.0.CO;2.

Marthews, T. R., et al. (2012), Simulating forest productivity along a neotropical elevational transect: Temperature variation and carbon use efficiency, *Global Change Biol.*, *18*(9), 2882–2898, doi:10.1111/j.1365-2486.2012.02728.x.

Martinez, J. M., J. L. Guyot, N. Filizola, and F. Sondag (2009), Increase in suspended sediment discharge of the Amazon River assessed by monitoring network and satellite data, *Catena*, *79*(3), 257–264, doi:10.1016/j.catena.2009.05.011.

Mayorga, E., A. K. Aufdenkampe, C. A. Masiello, A. V. Krusche, J. I. Hedges, P. D. Quay, J. E. Richey, and T. A. Brown (2005), Young organic matter as a source of carbon dioxide outgassing from Amazonian rivers, *Nature*, *436*(7050), 538–541, doi:10.1038/nature03880.

Mayorga, E., S. P. Seitzinger, J. A. Harrison, E. Dumont, A. H. W. Beusen, A. F. Bouwman, B. M. Fekete, C. Kroeze, and G. Van Drecht (2010), Global Nutrient Export from WaterSheds 2 (NEWS 2): Model development and implementation, *Environ. Modell. Software*, *25*(7), 837–853, doi:10.1016/j.envsoft.2010.01.007.

Meade, R. H., C. F. Nordin, W. F. Curtis, F. M. Costarodrigues, C. M. Dovale, and J. M. Edmond (1979), Sediment loads in the Amazon River, *Nature*, *278*(5700), 161–163.

Milliman, J. D. (1995), Sediment discharge to the ocean from small mountainous rivers: The New Guinea example, *Geo Mar. Lett.*, *15*(3–4), 127–133.

Milliman, J. D., and K. L. Farnsworth (2011), Runoff, erosion, and delivery to the coastal ocean, in *River Discharge to the Coastal Ocean: A Global Synthesis, edited*, pp. 13–69 , Cambridge Univ. Press, Cambridge, U. K.

Mitchard, E. T. A., et al. (2014), Markedly divergent estimates of Amazon forest carbon density from ground plots and satellites, *Global Ecol. Biogeogr.*, doi:10.1111/geb.12168.

Montgomery, D. R., G. Balco, and S. D. Willett (2001), Climate, tectonics, and the morphology of the Andes, *Geology*, *29*(7), 579–582, doi:10.1130/0091-7613(2001)029 < 0579:CTATMO > 2.0.CO;2.

Moreira-Turcq, L. S., P. Moreira Turcq, J. H. Kim, B. Turcq, R. C. Cordeiro, S. Caquineau, M. Mandengo-Yogo, and J. S. Sinninghe Damsté (2014), A mineralogical and organic geochemical overview of the effects of Holocene changes in Amazon River flow on three floodplain lakes, *Palaeogeogr. Palaeoclimatol. Palaeoecol.*, *415*, 152–164, doi:10.1016/j.palaeo.2014.03.017.

Moreira-Turcq, P., P. Seyler, J. L. Guyot, and H. Etcheber (2003), Exportation of organic carbon from the Amazon River and its main tributaries, *Hydrol. Process.*, *17*(7), 1329–1344, doi:10.1002/hyp.1287.

Moreira-Turcq, P., M.-P. Bonnet, M. Amorim, M. Bernardes, C. Lagane, L. Maurice, M. Perez, and P. Seyler (2013), Seasonal variability in concentration, composition, age, and fluxes of particulate organic carbon exchanged between the floodplain and Amazon River, *Global Biogeochem. Cycles*, *27*, 119–130, doi:10.1002/gbc.20022.

Petsch, S. (2014), Weathering of organic carbon, *Treatise Geochem.*, *12*, 217–238.

Petsch, S. T., R. A. Berner, and T. I. Eglinton (2000), A field study of the chemical weathering of ancient sedimentary organic matter, *Org. Geochem.*, *31*(5), 475–487, doi:10.1016/S0146-6380(00)00014-0.

Ponton, C., A. J. West, S. J. Feakins, and V. Galy (2014), Leaf wax biomarkers in transit record river catchment composition, *Geophys. Res. Lett.*, *41*, 6420–6427, doi:10.1002/2014GL061328.

Quay, P. D., D. O. Wilbur, J. E. Richey, J. I. Hedges, and A. H. Devol (1992), Carbon cycling in the Amazon River: Implications from the ^{13}C compositions of particles and solutes, *Limnol. Oceanogr.*, *37*(4), 857–871, doi:10.2307/2837944.

Ramos Scharrón, C. E., E. J. Castellanos, and C. Restrepo (2012), The transfer of modern organic carbon by landslide activity in tropical montane ecosystems, *J. Geophys. Res.*, *117*, G03016, doi:10.1029/2011JG001838.

Rao, Y. (2011), Variation in plant carbon and nitrogen isotopes along an altitudinal gradient in the Peruvian Andes, B.Sc. thesis, 60 pp., Department of Earth Sciences, Durham University, Durham.

Restrepo, C., L. R. Walker, A. B. Shiels, R. Bussmann, L. Claessens, S. Fisch, P. Lozano, G. Negi, L. Paolini, and G. Poveda (2009), Landsliding and its multiscale influence on mountainscapes, *BioScience*, *59*(8), 685–698, doi:10.1525/bio.2009.59.8.10.

Richey, J. E., R. H. Meade, E. Salati, A. H. Devol, C. F. Nordin, and U. Dossantos (1986), Water discharge and suspended sediment concentrations in the Amazon River, 1982–1984, *Water Resour. Res.*, *22*, 756–764, doi:10.1029/WR022i005p00756.

Richey, J. E., J. I. Hedges, A. H. Devol, P. D. Quay, R. Victoria, L. Martinelli, and B. R. Forsberg (1990), Biogeochemistry of carbon in the Amazon River, *Limnol. Oceanogr.*, *35*(2), 352–371.

Roering, J. J., J. W. Kirchner, and W. E. Dietrich (2001), Hillslope evolution by nonlinear, slope-dependent transport: Steady state morphology and equilibrium adjustment timescales, *J. Geophys. Res.*, *106*, 16,499–16,513, doi:10.1029/2001jb000323.

Rosenheim, B. E., and V. Galy (2012), Direct measurement of riverine particulate organic carbon age structure, *Geophys. Res. Lett.*, *39*, L198703, doi:10.1029/2012GL052883.

Rumpel, C., and I. Kögel-Knabner (2011), Deep soil organic matter—A key but poorly understood component of terrestrial C cycle, *Plant Soil*, *338*(1–2), 143–158, doi:10.1007/s11104-010-0391-5.

Saatchi, S. S., N. L. Harris, S. Brown, M. Lefsky, E. T. Mitchard, W. Salas, B. R. Zutta, W. Buermann, S. L. Lewis, and S. Hagen (2011), Benchmark map of forest carbon stocks in tropical regions across three continents, *Proc. Natl. Acad. Sci.*, *108*(24), 9899–9904, doi:10.1073/pnas.1019576108.

Schmidt, M. W. I., et al. (2011), Persistence of soil organic matter as an ecosystem property, *Nature*, *478*(7367), 49–56, doi:10.1038/nature10386.

Seitzinger, S. P., J. A. Harrison, E. Dumont, A. H. W. Beusen, and A. F. Bouwman (2005), Sources and delivery of carbon, nitrogen, and phosphorus to the coastal zone: An overview of Global Nutrient Export from Watersheds (NEWS) models and their application, *Global Biogeochem. Cycles*, *19*, GB4S01, doi:10.1029/2005GB002606.

Smith, J. C., A. Galy, N. Hovius, A. M. Tye, J. M. Turowski, and P. Schleppi (2013), Runoff-driven export of particulate organic carbon from soil in temperate forested uplands, *Earth Planet. Sci. Lett.*, *365*, 198–208, doi:10.1016/j.epsl.2013.01.027.

Stallard, R. F. (1998), Terrestrial sedimentation and the carbon cycle: Coupling weathering and erosion to carbon burial, *Global Biogeochem. Cycles*, *12*, 231–257, doi:10.1029/98gb00741.

Stallard, R. F. (2012), Weathering, landscape equilibrium, and carbon in four watersheds in eastern Puerto Rico: Chapter H, in *Water quality and landscape processes of four watersheds in eastern Puerto Rico*, edited by S. F. Murphy and R. F. Stallard, pp. 199–248, U.S. Geol. Surv. Prof. Pap., *1789*.

Stuiver, M., and H. A. Polach (1977), Discussion: Reporting of ^{14}C data, *Radiocarbon*, *19*(3), 355–363.

Sundquist, E., and K. Visser (2004), *The Geologic History of the Carbon Cycle*, pp. 425–472 , UK, Oxford.
Thomas, R. B. (1985), Estimating total suspended sediment yield with probability sampling, *Water Resour. Res.*, *21*, 1381–1388, doi:10.1029/WR021i009p01381.
Torres, M. A., A. J. West, and K. E. Clark (2015), Geomorphic regime modulates hydrologic control of chemical weathering in the Andes–Amazon, *Geochim. Cosmochim. Acta*, *166*, 105–128, doi:10.1016/j.gca.2015.06.007.
Torres, M. A., A. J. West, K. E. Clark, G. Paris, J. Bouchez, C. Ponton, S. J. Feakins, V. Galy, and J. Adkins (2016), The acid and alkalinity budgets of weathering in the Andes-Amazon system: Insights into the erosional control of global biogeochemical cycles?, *Earth Planet. Sci. Lett.*, *450*, 381–391, doi:10.1016/j.epsl.2016.06.012.
Townsend-Small, A., J. L. Noguera, M. E. McClain, and J. A. Brandes (2007), Radiocarbon and stable isotope geochemistry of organic matter in the Amazon headwaters, Peruvian Andes, *Global Biogeochem. Cycles*, *21*, GB2029, doi:10.1029/2006gb002835.
Townsend-Small, A., M. E. McClain, B. Hall, J. L. Noguera, C. A. Llerena, and J. A. Brandes (2008), Suspended sediments and organic matter in mountain headwaters of the Amazon River: Results from a 1-year time series study in the central Peruvian Andes, *Geochim. Cosmochim. Acta*, *72*, 732–740, doi:10.1016/j.gca.2007.11.020.
Turowski, J. M., A. Badoux, K. Bunte, C. Rickli, N. Federspiel, and M. Jochner (2013), The mass distribution of coarse particulate organic matter exported from an Alpine headwater stream, *Earth Surf. Dyn.*, *1*(1), 1–11, doi:10.5194/esurf-1-1-2013.
Turowski, J. M., R. G. Hilton, and R. Sparkes (2016), Decadal carbon discharge by a mountain stream is dominated by coarse organic matter, *Geology*, *44*(1), 27–30, doi:10.1130/G37192.1.
Vihermaa, L. E., S. Waldron, M. H. Garnett, and J. Newton (2014), Old carbon contributes to aquatic emissions of carbon dioxide in the Amazon, *Biogeosciences*, *11*(1), 3635–3645, doi:10.5194/bg-11-3635-2014.
Vihermaa, L. E., S. Waldron, T. Domingues, J. Grace, E. G. Cosio, F. Limonchi, C. Hopkinson, H. Ribeiro da Rocha, and E. Gloor (2016), Fluvial carbon export from a lowland Amazonian rainforest in relation to atmospheric fluxes, *J. Geophys. Res. Biogeosci.*, *121*, 3001–3018, doi:10.1002/2016JG003464.
Vogel, R. M., J. R. Stedinger, and R. P. Hooper (2003), Discharge indices for water quality loads, *Water Resour. Res.*, *39*(10), 1273, doi:10.1029/2002WR001872.
Walling, D. E., and B. W. Webb (1981), The reliability of suspended sediment load data, paper presented at Erosion and Sediment Transport Measurement, Proceedings from the Florence Symposium, June 1981, IAHS Publ. 133.
Wang, J., Z. Jin, R. G. Hilton, F. Zhang, A. L. Densmore, G. Li, and A. J. West (2015), Controls on fluvial evacuation of sediment from earthquake-triggered landslides, *Geology*, *43*(2), 115–118, doi:10.1130/G36157.1.
West, A. J., C. W. Lin, T. C. Lin, R. G. Hilton, S. H. Liu, C. T. Chang, K. C. Lin, A. Galy, R. B. Sparkes, and N. Hovius (2011), Mobilization and transport of coarse woody debris to the oceans triggered by an extreme tropical storm, *Limnol. Oceanogr.*, *56*(1), 77–85, doi:10.4319/lo.2011.56.1.0077.
Wheatcroft, R. A., M. A. Goni, J. A. Hatten, G. B. Pasternack, and J. A. Warrick (2010), The role of effective discharge in the ocean delivery of particulate organic carbon by small, mountainous river systems, *Limnol. Oceanogr.*, *55*(1), 161–171, doi:10.4319/lo.2010.55.1.0161.
Wittmann, H., F. von Blanckenburg, J. L. Guyot, L. Maurice, and P. Kubik (2009), From source to sink: Preserving the cosmogenic ^{10}Be-derived denudation rate signal of the Bolivian Andes in sediment of the Beni and Mamoré foreland basins, *Earth Planet. Sci. Lett.*, *288*(3), 463–474, doi:10.1016/j.epsl.2009.10.008.
Zimmermann, M., P. Meir, M. I. Bird, Y. Malhi, and A. J. Q. Ccahuana (2009), Climate dependence of heterotrophic soil respiration from a soil-translocation experiment along a 3000 m tropical forest altitudinal gradient, *Eur. J. Soil Sci.*, *60*(6), 895–906, doi:10.1111/j.1365-2389.2009.01175.x.
Zimmermann, M., P. Meir, M. I. Bird, Y. Malhi, and A. J. Q. Ccahuana (2010a), Temporal variation and climate dependence of soil respiration and its components along a 3000 m altitudinal tropical forest gradient, *Global Biogeochem. Cycles*, *24*, GB4012, doi:10.1029/2010GB003787.
Zimmermann, M., et al. (2010b), No differences in soil carbon stocks across the tree line in the Peruvian Andes, *Ecosystems*, *13*, 62–74, doi:10.1007/s10021-009-9300-2.